

NASA TECHNICAL NOTE



NASA TN D-4057

c.1

LOAN COPY: RETURN TO  
AFWL (WLIL-2)  
KIRTLAND AFB, N MEX



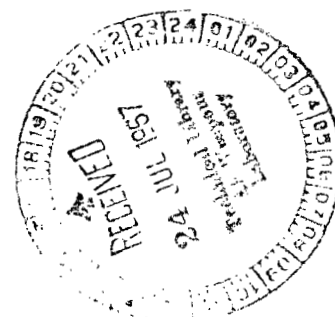
NASA TN D-4057

AN EXPERIMENTAL INVESTIGATION OF  
PRESSURE DROP AND HEAT TRANSFER FOR  
WATER BOILING IN A VERTICAL-UPFLOW  
SINGLE-TUBE HEAT EXCHANGER

*by James R. Stone and Thomas M. Damman*

*Lewis Research Center*

*Cleveland, Ohio*





AN EXPERIMENTAL INVESTIGATION OF PRESSURE DROP AND  
HEAT TRANSFER FOR WATER BOILING IN A VERTICAL-  
UPFLOW SINGLE-TUBE HEAT EXCHANGER

By James R. Stone and Thomas M. Damman

Lewis Research Center  
Cleveland, Ohio

NATIONAL AERONAUTICS AND SPACE ADMINISTRATION

---

For sale by the Clearinghouse for Federal Scientific and Technical Information  
Springfield, Virginia 22151 - CFSTI price \$3.00

# AN EXPERIMENTAL INVESTIGATION OF PRESSURE DROP AND HEAT TRANSFER FOR WATER BOILING IN A VERTICAL-UPFLOW SINGLE-TUBE HEAT EXCHANGER

by James R. Stone and Thomas M. Damman

Lewis Research Center

## SUMMARY

Experimental data were obtained on heat transfer and pressure drop for water boiling in the inner passage of a single-tube heat exchanger. The heating water flowed through the annular shell in either parallel or countercurrent flow. The heating water flow rate ranged from 2000 to 8500 pounds per hour (0.25 to 1.07 kg/sec), and its temperature ranged up to 348° F (449° K). Boiling fluid flow rates ranged from 50 to 870 pounds (mass) per hour (0.0063 to 0.11 kg/sec) or mass velocities from  $5.0 \times 10^4$  to  $8.7 \times 10^5$  pounds (mass) per hour per square foot (67 to 1200 kg/(sec)(m<sup>2</sup>)). Exit pressure from the boiler tube was varied from 3.5 to 24 pounds per square inch absolute (24 to 164 kN/m<sup>2</sup>). The highest heating rates obtained were 69 000 Btu per hour (20 200 W) in a 44.5-inch-long (1.13 m) tube and 118 000 Btu per hour (34 600 W) in a 60.5-inch-long (1.54 m) tube. The nominal inside diameter of each tube was 0.43 inch (1.1 cm).

Correlations were obtained of pressure drop and mean boiling-side heat-transfer coefficients. A slip-flow model was used to determine the mean two-phase friction factor from the experimental data. This friction factor was then correlated as a function of mean liquid and vapor Reynolds numbers.

Mean boiling-side heat-transfer coefficients were correlated for conditions under which the transition to dry-wall boiling did not occur. The ratio of the mean boiling-side heat-transfer coefficient to that for all-liquid turbulent flow was found to increase with increasing pressure and exit quality.

Limited data for the transition to dry-wall boiling were found to agree approximately with burnout data for water boiling in electrically heated tubes.

## INTRODUCTION

Rankine cycle systems with alkali metals as working fluids are of interest for use in

space power generation. Such systems would include two-phase heat-transfer components, namely, condensers and boilers. Two types of boilers are being considered; one in which the working fluid boils directly in the reactor and one in which the working fluid is boiled in a heat exchanger. With the heat-exchanger type, the heat supply liquid is heated by flowing through the reactor. In order to design such systems, data on boiler performance are required. This investigation is devoted to the performance of heat-exchanger boilers. Since experiments on the boiling of alkali metals are difficult and expensive to perform, this investigation of water-boiling heat exchangers was undertaken. The boiling pressures were held under 25 pounds per square inch absolute ( $170 \text{ kN/m}^2$ ), so that the liquid-to-vapor density ratio was of the magnitude to be expected for alkali metals in Rankine cycle space power systems.

Much information has been obtained on the boiling of water and other nonmetallic fluids, but most of it for boiling in electrically heated passages. Notable exceptions are the investigations by Dengler (ref. 1), Dengler and Addoms (ref. 2), Woods (ref. 3), and McAdams, Woods, and Bryan (ref. 4), wherein water was boiled in tubes heated by condensing steam. Similar data for the boiling of benzene are also given in reference 4.

Nucleate boiling has been studied by numerous investigators; some of these investigations are reviewed by Tong (ref. 5). Many sources of data for the convective boiling regime are also listed in reference 5. The correlations of references 6 to 8 are commonly used for the nucleate boiling regime. Correlations for heat-transfer in the convective boiling region are given in references 1, 2, and 9 to 15. These correlations predict different trends of the variation of the boiling heat-transfer coefficient with such variables as flow rate, quality, and physical properties.

Correlations of boiling pressure drops are also numerous. A number of these correlations are based on the early work of Lockhart and Martinelli (ref. 16), for example, those of references 17 and 18. The dimensional analysis of Lockhart and Martinelli (ref. 16) has also been applied to the correlation of heat-transfer data (refs. 1, 2, and 9 to 11). Levy (ref. 19) has proposed a momentum-exchange model, in which he postulated that as void fraction, quality and densities of the two-phase flow vary, momentum exchange equalizes the sum of frictional and gravitational head losses for the two phases. Thom (ref. 20) has developed a semiempirical correlation in which momentum, energy and mass balances are solved, assuming that the slip ratio (ratio of gas velocity to liquid velocity) is a function of the density ratio only. The two-phase friction factor was correlated as a function of quality.

Pressure-drop and heat-transfer data were obtained in this investigation for stainless-steel boiler tubes having 0.430 and 0.436 inch (1.09 and 1.11 cm) inside diameters and heated lengths of 44.5 and 60.5 inches (1.13 and 1.54 m) respectively. Boiling fluid flowrates ranged from 50 to 870 pounds (mass) per hour (0.0063 to 0.11 kg/sec) or mass velocities from  $5 \times 10^4$  to  $8.7 \times 10^5$  pounds (mass) per hour per square

foot (67 to 1200 kg/(sec)(m<sup>2</sup>)), at pressures from 3.5 to 24 pounds per square inch absolute (24 to 165 kN/m<sup>2</sup>), with heating fluid flow rates from 2000 to 8500 pounds (mass) per hour (0.25 to 1.07 kg/sec). Data were obtained on overall pressure drop through the boiler and mean boiling-side heat-transfer coefficients over the combined nucleate and convective boiling regimes. Limited data were also obtained on the transition to dry-wall boiling. The pressure drop data reported herein were correlated by a slip-flow model similar to that of Thom (ref. 20).

## APPARATUS

A schematic diagram of the test rig is shown in figure 1. The two-phase loop was the one described and used in reference 21, with the exception of the test section. The boiling fluid flow was supplied by a gear pump having a maximum output of 2 gallons per minute ( $1.25 \times 10^{-4}$  m<sup>3</sup>/sec). The flow was measured by one of the two turbine flowmeters having overlapping ranges. The flow then passed through a coiled stainless-steel electrical preheater. The maximum preheater power available was 70 kilowatts. The flow then passed through a remotely operated control valve into the test section. From the test section exit the flow passed through a 2-inch (5.1-cm) pipe to a spray condenser. The coolant was supplied to the condenser by a centrifugal pump having a nominal maximum capacity of 100 gallons per minute ( $6.3 \times 10^{-3}$  m<sup>3</sup>/sec). From the condenser the flow passed into a multiple-tube heat exchanger cooled by cooling-tower water. In most cases the condenser coolant pump was shut off and the condensing was done in the heat-exchanger cooler.

The heating fluid loop was designed for operation at pressures up to 200 pounds per square inch absolute (1400 kN/m<sup>2</sup>) and temperatures up to 350° F (450° K). The heating water was pumped by a centrifugal pump (4 to 20 gal/min or  $2.5 \times 10^{-4}$  to  $1.3 \times 10^{-3}$  m<sup>3</sup>/sec) into a tank equipped with an immersion heater, having a maximum output of 220 kilowatts. The heating-water flow through the test section could be changed from the countercurrent to the parallel flow direction by reversing the two connecting flexible lines (fig. 1). The heating fluid flowrate was measured by one of two turbine flowmeters having overlapping ranges.

A schematic test-section drawing is shown in figure 2. Both test sections consisted of two concentric stainless-steel tubes; the dimensions of the test sections are given in table I. The boiling fluid flow was vertically upward. For test section 2, boiler-tube inlet and exit pressures were measured by Bourdon-type gages as was the exit plenum pressure for both test sections. The gages were mounted at the same height as the pressure taps; the inlet and exit pressure gages of test section 2 were located less than 1 foot (0.4 m) from the taps. Thermocouples were inserted in both the inlet and exit

plenum chambers and in the heat supply inlet and exit lines. The shell-wall temperature was measured by 16 thermocouples spaced axially in the same plane. At three of these axial positions two other thermocouples were spaced  $120^\circ$  apart circumferentially around the tube. Thermocouples were imbedded in the inner-tube wall about 0.007 inch (0.18 mm); these thermocouples were then covered with a thin layer of cement to smooth the annular flow passage as shown in figure 2. The inner-tube wall thermocouples were used only to determine the onset of dry-wall boiling. There were 5 such thermocouples on test section 1 and 22 on test section 2. All of the thermocouples were copper constantan. The outer shells of the test sections were wrapped with a fiberglass insulating material.

## PROCEDURE

The dissolved-gas content of the water was maintained at about 3 parts per million by weight (or less) by venting the top of the condenser while boiling (method of determining gas content is discussed further in ref. 21). This was done each day before data were taken.

The conditions for each run were established by adjusting power to the main heater and preheater and setting the pump speeds and expansion tank pressures at selected values. When the inlet and exit temperatures became constant with time (or in some cases, slightly oscillatory), the data for that run were taken. In some cases the heating-fluid exit temperature oscillation was as much as  $\pm 2^\circ \text{F}$  ( $\pm 1.1^\circ \text{K}$ ), or 30 percent in heating rate. Temperatures were automatically recorded on strip charts. Flow rates and pressures were read from gages. Boiling-fluid flow oscillations greater than  $\pm 5$  percent are indicated in the tables. No data are presented for which the boiling-fluid flow oscillation was greater than  $\pm 10$  percent.

## DATA ANALYSIS

### Heat Loss Calibration

In order to determine the heat loss from the test section, a series of nonboiling runs was made. A heat balance was made between the two streams. The heat given up by the heating fluid was calculated from the following equation (Symbols are defined in the appendix.):

$$Q_H = W_H c_{PH} (T_{HI} - T_{HE}) \quad (1)$$

The heat gained by the coolant in the boiler tube was calculated from

$$Q = W_B c_{PL} (T_{BE} - T_{BI}) \quad (2)$$

An estimate of the heat loss to the ambient air indicated that such losses were negligible; therefore, the heat loss  $Q_L$ , where  $Q_L = Q_H - Q$ , was assumed to be due to end conduction losses. If the inlet and exit pipe lines were essentially at fluid temperature, the temperature difference between streams at each end of the test section might be an adequate indication of the driving potential for heat loss. Therefore, it was assumed that the sum of the heating-fluid-to-coolant temperature differences at the two ends of the boiler adequately represented the driving potential for such heat loss. The heat loss could be adequately represented by the empirical equation

$$Q_L = K [(T_{HI} - T_{BE}) + (T_{HE} - T_{BI})] \quad (3)$$

where  $K = 5.0$  Btu per hour per  $^{\circ}\text{F}$  ( $2.6 \text{ W}/^{\circ}\text{K}$ ). The heat loss  $Q_L$  was typically 2 to 4 percent of  $Q_H$ ; although for small values of  $Q_H$ ,  $Q_L$  approached 13 percent of  $Q_H$ . A comparison is made in figure 3 between the measured heating-fluid temperature drop (corrected for heat loss) and that computed from the coolant temperature rise. The average error in heating fluid temperature drop (corrected for heat loss) was 4 percent for temperature drops greater than  $4.5^{\circ}\text{F}$  ( $2.5^{\circ}\text{K}$ ) but increased to 9 percent for smaller temperature drops. If the flow measurements were accurate, the percentage error in  $Q$  would be the same as for  $\Delta T_H$ .

### Calculation of Tube-Side All-Liquid Heat-Transfer Coefficient

The tube-side all-liquid heat-transfer coefficient, required in subsequent calculations, was determined from reference 22. The ratio of local to fully developed heat-transfer coefficients is given therein as a function of  $Pr_L$ ,  $z/D$ , and  $L_U/D$ . The fully developed heat-transfer coefficient is correlated by a plot of  $(h_{fd}D/k_L)(DG/\mu_L)^{-0.8}$  as a function of  $Pr_L$ . The ratio  $h_{fd}/h(z)$ , the ratio of local to fully developed thermal resistances as calculated from reference 22, was plotted against  $z$  for several  $Pr_L$ . The ratio of the average thermal resistance,  $1/h_L$  to fully developed thermal resistance was found by graphical integration up to  $L_H/D$  for each test section. Plots of calcu-

lated values of  $(h_L D / k_L)(DG / \mu_L)^{-0.8}$  against  $Pr_L$  for each test section were found to well represented by the equation

$$\frac{h_L D}{k_L} = 0.023 \left( \frac{DG}{\mu_L} \right)^{0.8} Pr_L^{0.5} \quad (4)$$

### Determination of Thermal Resistance of Tube Wall and Heating-Fluid Stream

To determine the thermal resistance of the tube wall and the heating-fluid stream, the data from the nonboiling runs were again used. The average overall heat-transfer coefficient  $U$  was computed by the following equation for countercurrent runs:

$$U = \frac{\frac{Q}{S} \ln \left( \frac{T_{HE} - T_{BI}}{T_{HI} - T_{BE}} \right)}{(T_{HE} - T_{BI}) - (T_{HI} - T_{BE})} \quad (5)$$

For parallel-flow runs, the subscripts HE and HI must be interchanged. The mean tube-side heat-transfer coefficient was calculated from equation (4). Since the thermal resistances act in series, the combined resistance of the tube wall and heating-fluid film,  $R_o$  may be found from the equation

$$R_o = \frac{1}{U} - \frac{1}{h_L} \quad (6)$$

The wall resistance was assumed constant, while the heating-fluid film resistance was assumed to be proportional to the grouping  $(D_1 / k_H) Re_H^{-0.8} Pr_H^{-0.5}$ , where root-mean-square of properties at inlet and exit were used. The resistance  $R_o$  was then plotted against  $(D_1 / k_H) Re_H^{-0.8} Pr_H^{-0.5}$  for each test section as shown in figure 4. The results were correlated by equation (7a) for test section 1 and equation (7b) for test section 2, that is,

$$R_o = R_{w1} + 35.6 \left( \frac{D_1}{k_H} \right) Re_H^{-0.8} Pr_H^{-0.5} \quad (7a)$$

$$R_o = R_{w2} + 47 \left( \frac{D_1}{k_H} \right) Re_H^{-0.8} Pr_H^{-0.5} \quad (7b)$$



where the intercepts  $R_{w1}$  and  $R_{w2}$  are the tube-wall thermal resistances (approximately equal to wall thickness divided by thermal conductivity). Then  $R_{w1}$  is 0.00028 hour square foot  $^{\circ}\text{F}$  per Btu (0.000049  $(\text{M}^2)(^{\circ}\text{K})/\text{W}$ ), and  $R_{w2}$  is 0.00026 hour square foot  $^{\circ}\text{F}$  per Btu (0.000046  $(\text{M}^2)(^{\circ}\text{K})/\text{W}$ ). Values of  $U$  calculated from equation (5) were compared with values computed from equation (4), (6), and (7a) or (7b) in figure 5. It can be seen that for the nonboiling runs the mean overall heat-transfer coefficient agreed with the correlations to within less than 10 percent.

## Reduction of Thermal Data

For each boiling run the heating rate  $Q$  was computed from the following equation:

$$Q = Q_H - Q_L \quad (8)$$

where  $Q_H$  and  $Q_L$  were computed from equations (1) and (3), respectively. The exit vapor quality was calculated assuming thermodynamic equilibrium by the equation

$$x_E = \frac{Q}{W_B \lambda} - \frac{c_{Pl}}{\lambda} (T_{SE} - T_{BI}) \quad (9)$$

The enthalpy-weighted mean overall temperature difference was computed from

$$\Delta T_m = \overline{\Delta T}_{SC} \left[ \frac{W_B c_{Pl} (T_{SE} - T_{BI})}{Q} \right] + \overline{\Delta T}_B \left( \frac{x_E W_B \lambda}{Q} \right) \quad (10)$$

where  $\overline{\Delta T}_{SC}$  is the arithmetic-mean temperature difference from the boiler inlet to the point where the boiling-fluid bulk temperature reaches  $T_{SE}$  and  $\overline{\Delta T}_B$  is the arithmetic-mean temperature difference over the remaining length of the boiler. Utilizing an enthalpy-weighted mean temperature difference, as opposed to length weighted, allows calculations to be made without first estimating the temperature distributions. Based on this mean temperature difference, the overall mean heat-transfer coefficient was computed from the following equation:

$$U = \frac{Q}{S \Delta T_m} \quad (11)$$

The thermal resistance of the tube wall and heating fluid was computed from equation (7a)

or (7b). Thus the mean boiling-side heat-transfer coefficient was computed from

$$h_B = \frac{1}{\frac{1}{U} - R_o} \quad (12)$$

## Pressure Drop Calculations

Application of the laws of conservation of energy, mass, and momentum yields the pressure drop as the sum of three terms - inertial, frictional, and gravitational. The results of Thom (ref. 20) for constant heat flux, friction factor, and physical properties are given as

$$\Delta P_I = \frac{G^2}{g_c \rho_l} \left\{ \left[ 1 + x_E \left( \frac{1}{V} \frac{\rho_l}{\rho_g} - 1 \right) \right] \left[ 1 + x_E (V - 1) \right] - 1 \right\} \quad (13a)$$

$$\Delta P_F = \frac{f_{TP} G^2 L_H}{g_c \rho_l D} \left\{ \left[ 1 + x_E \left( \frac{1}{V} \frac{\rho_l}{\rho_g} - 1 \right) \right] \left[ 1 + x_E (V - 1) \right] + 1 \right\} \quad (13b)$$

$$\Delta P_G = \rho_l L_H \left( \frac{g}{g_c} \right) \left\{ \frac{\frac{1}{V} - 1}{\frac{1}{V} \frac{\rho_l}{\rho_g} - 1} + \frac{\frac{1}{V} \frac{\rho_l}{\rho_g} - \frac{1}{V}}{\left( \frac{1}{V} \frac{\rho_l}{\rho_g} - 1 \right)^2} \frac{\ln \left[ 1 + x_E \left( \frac{1}{V} \frac{\rho_l}{\rho_g} - 1 \right) \right]}{x_E} \right\} \quad (13c)$$

In the previous equations  $V$  is the ratio of mean gas velocity to mean liquid velocity. The inertial pressure drop  $\Delta P_I$  is a function of the mean density and velocity at the inlet and at the exit and is independent of the local heat flux distribution within the boiler. Uniform heat flux was assumed in order to obtain the frictional and gravitational pressure drop equations (eqs. (13b) and (13c)). Since the heat flux was not necessarily uniform and the two-phase friction factor  $f_{TP}$  was not necessarily constant (as is assumed in the integration), the experimental values of  $f_{TP}$  are effective mean values. The gravitational pressure drop  $\Delta P_G$  generally is relatively small. Since the inception of boiling was very near the inlet for nearly all of the data, the total heated length is used in equations (13b) and (13c).

In order to use equations (13), the parameter  $V$  must be known. In correlating the

data it was found by trial and error that the approximation  $V = \sqrt{\rho_l/\rho_g}$  appears valid. Although this is different from the relation between velocity ratio and density ratio used in reference 20, it should be noted that the correlation obtained therein is applied only to the pressure range well above 200 pounds per square inch absolute ( $1.4 \times 10^6$  N/m<sup>2</sup>).

The pressure drop equations (eqs. (13)) may be combined, assuming  $V = \sqrt{\rho_l/\rho_g}$ , to yield the following:

$$\Delta P = \frac{G^2}{\rho_l g_c} \left\{ \left[ 1 + x_E \left( \sqrt{\frac{\rho_l}{\rho_g}} - 1 \right) \right]^2 - 1 + f_{TP} \frac{L_H}{D} \left[ \left\langle 1 + x_E \left( \sqrt{\frac{\rho_l}{\rho_g}} - 1 \right) \right\rangle^2 + 1 \right] \right\} \\ + \rho L_H \left( \frac{g}{g_c} \right) \left\{ \frac{\sqrt{\frac{\rho_g}{\rho_l}} - 1}{\sqrt{\frac{\rho_l}{\rho_g}} - 1} + \frac{\left( \sqrt{\frac{\rho_l}{\rho_g}} - \sqrt{\frac{\rho_g}{\rho_l}} \right) \ln \left[ 1 + x_E \left( \sqrt{\frac{\rho_l}{\rho_g}} - 1 \right) \right]}{x_E \left( \sqrt{\frac{\rho_l}{\rho_g}} - 1 \right)^2} \right\} \quad (14)$$

Or more simply

$$\Delta P = \frac{G^2}{\rho_l g_c} \left[ R_1 + f_{TP} \left( \frac{L_H}{D} \right) (R_1 + 2) \right] + R_2 \left( \frac{g}{g_c} \right) \rho_l L_H \quad (14a)$$

where

$$R_1 = \left[ 1 + x_E \left( \sqrt{\frac{\rho_l}{\rho_g}} - 1 \right) \right]^2 - 1 \quad (14b)$$

and

$$R_2 = \frac{\sqrt{\frac{\rho_g}{\rho_l}} - 1}{\sqrt{\frac{\rho_l}{\rho_g}} - 1} + \frac{\left( \sqrt{\frac{\rho_l}{\rho_g}} - \sqrt{\frac{\rho_g}{\rho_l}} \right) \ln \left[ 1 + x_E \left( \sqrt{\frac{\rho_l}{\rho_g}} - 1 \right) \right]}{x_E \left( \sqrt{\frac{\rho_l}{\rho_g}} - 1 \right)^2} \quad (14c)$$

For convenience, the multipliers  $R_1$  and  $R_2$  are plotted against  $x_E$  for various values of  $\rho_l/\rho_g$  in figures 6 and 7, respectively.

To determine the two-phase friction factor from the experimental data, equation (14) may be solved for  $f_{TP}$  as follows:

$$f_{TP} = \frac{\Delta P - R_2 \rho_l \left( \frac{g}{g_c} \right) L_H - \frac{R_1 G^2}{\rho_l g_c}}{(R_1 + 2) \frac{L_H G^2}{D \rho_l g_c}} \quad (15)$$

## RESULTS AND DISCUSSION

Single-tube heat exchanger boiling data on pressure drop, heat transfer, and the onset of dry-wall boiling are presented and discussed in this section. Comparisons are made with other water data and with alkali-metal data.

### Tabulation of Data

The basic experimental data are tabulated in table II. Tabulated therein are the flow rates, inlet and exit temperatures for both streams, the heating rate, exit quality, boiler exit pressure, and the critical length (the boiler-tube length to the point where a large rise in wall temperature was observed). The tabulated boiling-fluid exit temperature is the saturation temperature at the boiler exit pressure, since there was a noticeable pressure drop through the exit plenum chamber, especially at subatmospheric pressures. The boiler inlet pressure is also tabulated for test section 2 only.

### Pressure Drop

The semi-empirical, slip-flow model presented in the section Pressure Drop Calculations was used to evaluate two-phase friction factors from experimental pressure drop data. The pressure drop data presented herein, the data of Dengler (ref. 1) for water in upflow through a 20-foot (6.1-m) high, 1-inch (2.5-cm) inside diameter steam-heated boiler, and some unpublished NASA sodium boiling data were examined. It was found that the two-phase friction factor could be correlated as a function of mean liquid and gas Reynolds numbers, defined as follows:

$$\text{Re}_l = \frac{DG}{\mu_l} \left( 1 - \frac{x_E}{2} \right) \quad (16a)$$

$$\text{Re}_g = \frac{DG}{\mu_g} \frac{x_E}{2} \quad (16b)$$

It was assumed that the variation of  $f_{\text{TP}}$  with the gas Reynolds number is given by  $f_{\text{TP}} \sim \text{Re}_g^{-0.2}$ . Therefore,  $f_{\text{TP}} \text{Re}_g^{0.2}$  was plotted against  $\text{Re}_l$  as in figure 8. The data may be correlated by the following equation:

$$f_{\text{TP}} = 0.020 \text{Re}_g^{-0.2} (1 + 0.027 \text{Re}_l^{0.5}) \quad (17)$$

Values of  $\Delta P$  calculated from equations (14), (16), and (17) are compared with the experimentally observed values in figure 9. The agreement is within  $\pm 20$  percent for  $\Delta P$  greater than 7 pounds per square inch ( $50 \text{ kN/m}^2$ ) with the agreement being poorer for smaller pressure drops.

## Heat Transfer

Experimental values of the mean boiling-side heat-transfer coefficient are plotted against exit quality for various boiler flow rates at an exit pressure of approximately 17 pounds per square inch absolute ( $115 \text{ kN/m}^2$ ) in figure 10. It can be seen that  $h_B$  increases strongly with flowrate and exit quality (provided that transition to dry-wall boiling did not occur). This increase of  $h_B$  with flow and quality indicates that the dominant mechanism may be of a convective nature. The effect of flowrate can be approached by assuming that  $h_B$  is proportional to  $h_L$ , the coefficient for all liquid flow at the same total flow rate and temperature. This is shown in figure 11, where  $h_B/h_L$  is plotted against  $x_E$  for exit pressures of approximately 8 and 17 pounds per square inch absolute. The mean boiling-side heat-transfer coefficient increases with increasing pressure for a given flow rate and exit quality even though the vapor velocity would tend to decrease due to the increasing vapor density. This increase of heat-transfer coefficient with pressure has also been observed in unpublished alkali-metal data. The effect of pressure may be correlated by plotting  $h_B/h_L$  against  $x_E (P_E/P_C)^{0.5}$ , where  $P_C$  is the critical pressure, as shown in figure 12; the data shown are those presented herein and those of Dengler (ref. 1). The data may be correlated as follows, so long as dry-wall boiling does not occur, for exit qualities greater than

$$1.5 \ c_{Pl}(T_{SE} - T_{BI})/\lambda:$$

$$\frac{h_B}{h_L} = 1 + 200 \ x_E \sqrt{\frac{P_E}{P_C}} \quad (18)$$

It is believed that subcooled boiling effects cause discrepancies at lower exit qualities, for the range of variables tested herein. The data correlated are for  $P_E/P_C$  from  $10^{-3}$  to  $10^{-2}$  approximately. Since the properties involved are uncertain, extrapolation is uncertain.

Mean overall heat-transfer coefficients were calculated from equations (18), (7a) or (7b), and (6) and compared with the experimental values in figure 13, where  $U_{calc}/U_{exp}$  is plotted against the temperature drop in the heating fluid. Since  $\Delta T_H$  is considered the most error-prone measurement, poorer accuracy is to be expected for small  $\Delta T_H$ . The agreement is within  $\pm 11$  percent for  $\Delta T_H$  greater than  $9^\circ \text{ F}$  ( $5^\circ \text{ K}$ ) and is poorer for smaller values of  $\Delta T_H$ .

### Critical Quality Data

The range of conditions for which the transition to dry-wall regimes occurred was too small to attempt a correlation of the data. A comparison is made in figure 14 with the burnout data of Lowdermilk, et al. (ref. 23). The curve plotted represents burnout data for electrically heated tubes, with a length-to-diameter ratio of 150 (diameters from 0.051 to 0.188 in. or 1.30 to 4.78 mm), an inlet temperature of about  $70^\circ \text{ F}$  ( $295^\circ \text{ K}$ ), and an exit pressure of about 15 pounds per square inch absolute ( $100 \text{ kN/m}^2$ ). Exit quality is plotted against the flow parameter  $GD$  for the data of test section 2 ( $L_H/D = 139$ ). Tails on the data points indicate that a large rise in inner-tube wall temperature was observed, indicating dry-wall boiling. The fact that the curve approximately marks the dividing line between tailed and untailed points indicates good comparison between the onset of dry-wall boiling in a heat exchanger and burnout in electrically heated tubes. (This is not intended to be a general correlation.) The agreement between these two sets of data is reasonably good except for the lowest flow rates for the heat exchanger. It is believed that this disagreement was due to instability, as considerable flow oscillations occurred at low flow rates with high exit quality.

## SUMMARY OF RESULTS

The results of this investigation of the pressure drop and heat transfer for water boiling in a vertical single-tube heat exchanger may be summarized as follows:

1. Data on heat transfer, pressure drop, and the transition from convective to dry-wall boiling are tabulated for pressures from 3.5 to 24 pounds per square inch absolute (24 to 165 kN/m<sup>2</sup>).

2. A slip-flow model similar to that of Thom was used to correlate the pressure drop data. The ratio of mean gas-phase to liquid-phase velocities was assumed equal to the square root of the liquid-to-gas density ratio. The mean two-phase friction factor was then correlated as a function of mean liquid and vapor Reynolds numbers. Some unpublished NASA sodium boiling data and Dengler's data for water were shown to agree with this correlation.

3. Mean boiling-side heat-transfer coefficients were correlated for conditions in which the transition to dry-wall boiling did not occur. The ratio of mean boiling-side heat-transfer coefficient to that for all-liquid turbulent flow was found to increase with increasing pressure and exit quality.

4. Data on the transition to dry-wall boiling were shown to agree roughly with the burnout data of Lowdermilk, et al. for water flowing through electrically heated tubes, so long as flow oscillations were avoided.

Lewis Research Center,  
National Aeronautics and Space Administration,  
Cleveland, Ohio, March 20, 1967,  
120-27-02-03-22.

## APPENDIX - NOMENCLATURE

A	cross-sectional area of boiling-fluid passage, $\text{ft}^2$ ( $\text{m}^2$ )	$h_L$	mean tube-side heat-transfer coefficient for all-liquid turbulent flow, $\text{Btu}/(\text{hr})(\text{ft}^2)(^\circ\text{F})$ ( $\text{W}/(\text{m}^2)(^\circ\text{K})$ )
$A_1$	cross-sectional area of heating-fluid passage, $\text{ft}^2$ ( $\text{m}^2$ )	K	constant in eq. (3), $\text{Btu}/(\text{hr})(^\circ\text{F})$ ( $\text{W}/^\circ\text{K}$ )
$c_{PH}$	heat capacity at constant pressure for heating fluid, $\text{Btu}/(\text{lb}_m)(^\circ\text{F})$ ( $\text{J}/(\text{kg})(^\circ\text{K})$ )	$k_H$	thermal conductivity of heating fluid, $\text{Btu}/(\text{hr})(\text{ft})(^\circ\text{F})$ ( $\text{W}/(\text{m})(^\circ\text{K})$ )
$c_{PL}$	liquid heat capacity at constant pressure for boiling fluid, $\text{Btu}/(\text{lb}_m)(^\circ\text{F})$ ( $\text{J}/(\text{kg})(^\circ\text{K})$ )	$k_L$	liquid thermal conductivity of boiling fluid, $\text{Btu}/(\text{hr})(\text{ft})(^\circ\text{F})$ ( $\text{W}/(\text{m})(^\circ\text{K})$ )
D	inside diameter of boiler tube, ft (m)	L	length of boiler tube, ft (m)
$D_o$	outside diameter of shell tube, ft (m)	$L_C$	distance from start of heating to point of transition from convective to dry-wall boiling, ft (m)
$D_1$	outside diameter of boiler tube, ft (m)	$L_H$	heated length of boiler, ft (m)
$D_2$	inside diameter of shell tube, ft (m)	$L_U$	length of unheated section at each end of boiler, ft (m)
$f_{TP}$	two-phase friction factor	$\Delta P$	pressure drop across boiler, psi ( $\text{kN}/\text{m}^2$ )
G	mass velocity of boiling fluid, $\text{lb}_m/(\text{hr})(\text{ft}^2)$ ( $\text{kg}/(\text{sec})(\text{m}^2)$ )	$P_C$	thermodynamic critical pressure psia ( $\text{kN}/\text{m}^2(\text{abs})$ )
g	acceleration due to gravity, $4.17 \times 10^8 \text{ ft/hr}^2$ ( $9.81 \text{ m/sec}^2$ )	$P_E$	boiler exit pressure, psia ( $\text{kN}/\text{m}^2(\text{abs})$ )
$g_c$	conversion factor, $4.17 \times 10^8$ ( $\text{ft})(\text{lb}_m)/(\text{lb}_f)(\text{hr}^2)$ ( $(1.00 \text{ (m)})(\text{kg})/(\text{N})(\text{sec}^2)$ )	$\Delta P_F$	frictional pressure drop, psi ( $\text{kN}/\text{m}^2$ )
h	heat-transfer coefficient, $\text{Btu}/(\text{hr})(\text{sq ft})(^\circ\text{F})$ ( $(\text{W}/(\text{m}^2)(^\circ\text{K}))$ )	$\Delta P_G$	gravitational pressure drop, psi ( $\text{kN}/\text{m}^2$ )
$h_B$	mean boiling-side heat-transfer coefficient, $\text{Btu}/(\text{hr})(\text{ft}^2)(^\circ\text{F})$ ( $\text{W}/(\text{m}^2)(^\circ\text{K})$ )	$\Delta P_I$	inertial pressure drop, psi ( $\text{kN}/\text{m}^2$ )



$Pr_H$	Prandtl number of heating fluid, dimensionless	$S_1$	outer heated surface area of boiler tube, $ft^2$ ( $m^2$ )
$Pr_l$	liquid Prandtl number of boiling fluid, dimensionless	$T$	temperature, $^{\circ}F$ ( $^{\circ}K$ )
$Q$	heating rate, Btu/hr (W)	$\Delta T_H$	temperature lost by heating fluid, $^{\circ}F$ ( $^{\circ}K$ )
$Q_H$	heat given up by heating fluid, Btu/hr (W)	$\Delta T_m$	mean temperature difference, $^{\circ}F$ ( $^{\circ}K$ )
$Q_L$	heat loss from test section to surroundings, Btu/hr (W)	$\overline{\Delta T_B}$	arithmetic-mean temperature difference across net boiling region, $^{\circ}F$ ( $^{\circ}K$ )
$R_o$	thermal resistance of boiler tube wall and heating fluid, $(hr)(ft^2)(^{\circ}F)/Btu$ $((m^2)(^{\circ}K)/W)$	$\overline{\Delta T_{SC}}$	arithmetic-mean temperature difference across subcooled region, $^{\circ}F$ ( $^{\circ}K$ )
$R_{w1}$	thermal resistance of boiler tube wall of test section 1, $(hr)(ft^2)(^{\circ}F)/Btu$ $((m^2)(^{\circ}K)/W)$	$U$	mean overall heat-transfer coefficient, $Btu/(hr)(ft^2)(^{\circ}F)$ $(W/(m^2)(^{\circ}K))$
$R_{w2}$	thermal resistance of boiler tube wall of test section 2, $(hr)(ft^2)(^{\circ}F)/Btu$ $((m^2)(^{\circ}K)/W)$	$V$	ratio of gas to liquid velocities, dimensionless
$R_1$	slip-flow parameter (fig. 6), dimensionless	$W_B$	flow rate of boiling fluid, $lb_m/hr$ ( $kg/sec$ )
$R_2$	gravitational pressure drop multiplier (fig. 7), dimensionless	$W_H$	flow rate of heating fluid, $lb_m/hr$ ( $kg/sec$ )
$Re_g$	mean gas Reynolds number (eq. (16b)), dimensionless	$x_E$	boiler exit quality, dimensionless
$Re_H$	mean heating-fluid Reynolds number, $4W_H/\pi(D_1 + D_2)\mu$	$z$	axial distance from start of heating, ft (m)
$Re_l$	mean liquid Reynolds number (eq. (16a)), dimensionless	$\delta$	thickness of boiler tube wall, ft (m)
$S$	inner heated surface area of boiler tube, $ft^2$ ( $m^2$ )	$\lambda$	heat of vaporization, $Btu/lb_m$ ( $J/kg$ )
		$\mu$	viscosity, $lb_m/(ft)(hr)$ ( $kg/(m)(sec)$ )
		$\rho$	density, $lb_m/ft^3$ ( $kg/m^3$ )

**Subscripts:**

BE     boiling-fluid exit  
BI     boiling-fluid inlet  
calc   calculated  
exp    experimental  
fd     fully developed

g       gas property  
HE     heating-fluid exit  
HI     heating-fluid inlet  
l       liquid property  
SE     saturation at boiler exit

## REFERENCES

1. Dengler, Carl E.: Heat Transfer and Pressure Drop for Evaporation of Water in a Vertical Tube. Ph.D. Thesis, Massachusetts Institute of Technology, 1952.
2. Dengler, C. E.; and Addoms, J. N.: Heat Transfer Mechanism for Vaporization of Water in a Vertical Tube. AIChE Chem. Eng. Progr. Symp. Ser., vol. 52, no. 18, 1956, pp. 95-103.
3. Woods, W. K.: Heat Transfer for Boiling Inside Horizontal Tubes. D.Sc. Thesis, Massachusetts Inst. Tech., 1940.
4. McAdams, W. H.; Woods, W. K.; and Bryan, R. L.: Vaporization Inside Horizontal Tubes. ASME Trans., vol. 63, no. 6, Aug. 1941, pp. 545-552.
5. Tong, L. S.: Boiling Heat Transfer and Two-Phase Flow. John Wiley and Sons, Inc., 1965.
6. Forster, H. K.; and Zuber, N.: Dynamics of Vapor Bubbles and Boiling Heat Transfer. AIChE J. vol. 1, no. 4, Dec. 1955, pp. 531-535.
7. Engelberg-Forster, Kurt; and Greif, R.: Heat Transfer to a Boiling Liquid - Mechanism and Correlations. J. Heat Transfer, vol. 81, no. 1, Feb. 1959, pp. 43-53.
8. Bergles, A. E.; and Rohsenow, W. M.: The Determination of Forced-Convection Surface-Boiling Heat Transfer. J. Heat Transfer, vol. 86, no. 3, Aug. 1964, pp. 365-372.
9. Schrock, V. E.; and Grossman, L. M.: Forced Convection Boiling Studies. AEC Rep. No. TID-14632, University of California, Lawrence Radiation Lab., Nov. 1, 1959.
10. Wright, Roger M.: Downflow Forced-Convection Boiling of Water in Uniformly Heated Tubes. Rep. No. UCRL-9744, University of California, Aug. 21, 1961.
11. Collier, J. G.; and Pulling, D. J.: Heat Transfer to Two-Phase Gas-Liquid Systems, Part II: Further Data on Steam-Water Mixtures. Rep. No. AERE-R-3809, United Kingdom Atomic Energy Authority, 1962.
12. Mumm, J. F.: Heat Transfer to Boiling Water Forced Through a Uniformly Heated Tube. Rep. No. ANL-5276, Argonne National Lab., Nov. 1954.
13. Altman, M.; Norris, R. H.; and Staub, F. W.: Local and Average Heat Transfer and Pressure Drop for Refrigerants Evaporating in Horizontal Tubes. J. Heat Transfer, vol. 82, no. 3, Aug. 1960, pp. 189-198.

14. Sachs, P.; and Long, R. A. K.: A Correlation for Heat Transfer in Stratified Two-Phase Flow with Vaporization. *Int. J. Heat Mass Transfer*, vol. 2, no. 3, Apr. 1961, pp. 222-230.
15. Chen, John C.: A Correlation for Boiling Heat Transfer to Saturated Fluids in Convective Flow. Paper No. 63-HT-34, ASME, 1963.
16. Lockhart, R. W.; and Martinelli, R. C.: Proposed Correlation of Data for Isothermal Two-Phase, Two-Component Flow in Pipes. *Chem. Eng. Progr.*, vol. 45, no. 1, Jan. 1949, pp. 39-48.
17. Martinelli, R. C.; and Nelson, D. B.: Prediction of Pressure Drop During Forced-Circulation Boiling of Water. *ASME Trans.*, vol. 70, no. 6, Aug. 1948, pp. 695-702.
18. Schrock, V. E.; and Grossman, L. M.: Local Pressure Gradients in Forced Convection Vaporization. *Nucl. Sci. Eng.*, vol. 6, no. 3, Sept. 1959, pp. 245-250.
19. Levy, S.: Steam Slip-Theoretical Prediction from Momentum Model. *J. Heat Transfer*, vol. 80, no. 2, May 1960, pp. 113-124.
20. Thom, J. R. S.: Prediction of Pressure Drop During Forced Circulation Boiling of Water. *Int. J. Heat Mass Transfer*, vol. 7, no. 7, July 1964, pp. 709-724.
21. Jeglic, Frank A.; Stone, James R.; and Gray, Vernon H.: Experimental Study of Subcooled Nucleate Boiling of Water Flowing in 1/4-Inch-Diameter Tubes at Low Pressures. NASA TN D-2626, 1965.
22. Stone, James R.: Local Turbulent Heat Transfer for Water in Entrance Regions of Tubes with Various Unheated Starting Lengths. NASA TN D-3098, 1965.
23. Lowdermilk, Warren H.; Lanzo, Chester D.; and Siegel, Byron L.: Investigation of Boiling Burnout and Flow Stability for Water Flowing in Tubes. NACA TN 4382, 1958.

TABLE I. - TEST-SECTION DIMENSIONS

Dimension	Test section	
	1	2
Total length of boiler tube, L, ft (m)	4.00 (1.22)	5.33 (1.63)
Insulated length (each end), $L_U$ , ft (cm)	0.146 (4.45)	0.146 (4.45)
Heated length, $L_H$ , ft (m)	3.71 (1.13)	5.04 (1.54)
Inner diameter of boiler tube, D, ft (cm)	0.0358 (1.09)	0.0363 (1.11)
Outer diameter of boiler tube, $D_1$ , ft (cm)	0.0417 (1.27)	0.0417 (1.27)
Inner diameter of shell tube, $D_2$ , ft (cm)	0.0833 (2.54)	0.0833 (2.54)
Outer diameter of shell tube, $D_O$ , ft (cm)	0.0937 (2.86)	0.0937 (2.86)
Boiler tube wall thickness, $\delta$ , ft (cm)	0.0029 (0.0089)	0.0027 (0.0081)
Inner heated surface area of boiler tube, S, $\text{ft}^2$ ( $\text{m}^2$ )	0.417 (0.0388)	0.576 (0.0535)
Outer heated surface area of boiler tube, $S_1$ , $\text{ft}^2$ ( $\text{m}^2$ )	0.485 (0.0450)	0.660 (0.0614)
Cross-sectional area of boiler tube, A, $\text{ft}^2$ ( $\text{m}^2$ )	0.00101 ( $9.40 \times 10^{-5}$ )	0.00104 ( $9.63 \times 10^{-5}$ )
Cross-sectional area of annulus, $A_1$ , $\text{ft}^2$ ( $\text{m}^2$ )	0.00409 ( $3.80 \times 10^{-4}$ )	0.00409 ( $3.80 \times 10^{-4}$ )

TABLE II. - EXPERIMENTAL DATA

(a) Test section 1 - countercurrent flow

Run	Boiling fluid									Heating rate, Q		Critical length, <sup>a</sup> L <sub>C</sub>		Heating fluid					
	Flow rate, W <sub>B</sub>		Inlet temperature, T <sub>BI</sub>		Exit temperature, T <sub>BE</sub>		Exit pressure, P <sub>E</sub>		Exit quality, x <sub>E</sub>					Flow rate, W <sub>H</sub>		Inlet temper- ature, T <sub>HI</sub>		Exit temper- ature, T <sub>HE</sub>	
	lb <sub>m</sub> hr	kg sec	°F	°K	°F	°K	psia	kN m <sup>2</sup> (abs)		Btu hr	kW	ft	m	lb <sub>m</sub> hr	kg sec	°F	°K	°F	°K
1	50	0.0063	84	302	216.5	375.6	16.0	110	0.08	10 000	3.0	----	----	2060	0.260	250	394.3	245.5	391.3
2	52	.0065	91	306	218.5	376.8	16.6	114	.26	19 300	5.7	----	----	1960	.247	294.5	419	284	413.2
3	51	.0064	96	308.7	218.5	376.8	16.6		.67	39 500	11.6	----	----	1980	.250	340	444.8	320	433.2
4	50	.0063	105	313.7	218	376.5	16.5		.74	41 400	12.1	2.50	0.762	2450	.309	344	446.5	327	437
5	b <sub>50</sub>	.0063	105	313.7	218.5	376.8	16.6	↓	.80	44 400	13.0	2.50	.762	2950	.372	346	447.6	331	439.3
6	b <sub>49</sub>	.0062	107	314.8	218.5	376.8	16.6	114	.88	47 200	13.8	2.50	0.762	3350	.442	346	447.6	332	439.8
7	b <sub>51</sub>	.0064	109	316	↓	↓	↓	↓	.80	44 700	13.1	↓	↓	3710	.468	346	447.6	334	441
8	b <sub>51</sub>	.0064	109	316	↓	↓	↓	↓	.87	48 300	14.2			4170	.525	345.5	447.3	334	441
9	b <sub>50</sub>	.0063	112	317.6	↓	↓	↓	↓	.88	47 800	14.0	1.83	.559	4500	.567	346	447.6	335.5	441.8
10	b <sub>50</sub>	.0063	114	318.7	↓	↓	↓	↓	.80	43 600	12.8	2.50	.762	4340	.547	345.5	447.3	335.5	441.8
11	b <sub>50</sub>	.0063	115	319.3	218	376.5	16.4	113	.95	51 000	15	1.83	.559	5610	.708	343	445.9	334	441
12	b <sub>51</sub>	.0064	117	320.4	218.5	376.8	16.6	114	1.0	56 000	16	2.50	.762	6130	.762	343	445.9	334	441
13	b <sub>50</sub>	.0063	118	321	218.5	376.8	16.7	115	.76	42 000	12	2.50	.762	6900	.870	343	445.9	337	442.6
14	b <sub>50</sub>	.0063	118	321	219	377	16.8	116	.91	49 000	14	2.50	.762	8450	1.07	342.5	445.6	337	442.6
15	45	.0057	122	323.2	216.5	375.6	16.0	110	.98	47 000	14	1.83	.559	8450	1.07	330	438.7	324.5	435.6
16	b <sub>53</sub>	.0067	114	318.7	217.5	376.2	16.3	112	.98	55 000	16	2.50	.762	8450	1.07	328.5	437.9	322	434.3
18	b <sub>63</sub>	.0079	112	317.6	217.5	376.2	16.3	112	.88	60 000	18	3.17	.966	8500	1.07	329.5	438.4	322.5	434.5
19	b <sub>67</sub>	.0084	85	302.6	218.5	376.7	16.7	115	.22	22 800	6.7	----	----	2150	.271	305	424.8	294	418.7
20	67	.0084	88	304.3	218	376.5	16.4	113	.33	29 700	8.7	----	----	2090	.263	322	434.3	307.5	426.2
21	67	.0084	91	306	218	376.5	16.4	113	.49	40 300	11.8	----	----	2180	.275	343	445.9	324.5	435.6
22	b <sub>82</sub>	.0103	193	362.6	219.5	377.3	17.0	117	.39	32 500	9.5	----	----	2170	.273	315	430.4	300	422
23	78	.0098	180	355.4	219	377	16.9	116	.85	67 000	20	3.17	.966	8700	1.10	332	439.8	324.5	435.6
24	80	.0101	180	355.4	219	377	16.9	116	.70	57 000	17	(c)	(c)	8630	1.08	335.5	441.8	329	438.2
25	b <sub>82</sub>	.0103	102.5	312.3	220	377.6	17.1	118	.69	64 000	19	2.50	.762	8450	1.06	344	446.5	336.5	442.3
26	81	.0102	102.5	312.3	218.5	376.7	16.7	115	.77	69 000	20	1.83	.559	8520	1.07	329.5	438.4	321.5	434
27	b <sub>73</sub>	.0092	110	316.5	218	376.5	16.4	113	.80	64 000	19	1.83	.559	8520	1.07	330	438.7	322.5	434.5
28	96	.0121	84	302	218.5	376.7	16.6	114	.12	23 500	6.9	----	----	2160	.272	305	424.8	294	418.7
29	96	.0121	87	303.7	218.5	376.7	16.6	114	.20	31 400	9.2	----	----	2130	.268	322	434.3	307	425.9
30	96	.0121	89	304.8	218	376.5	16.4	113	.29	39 500	11.6	----	----	2140	.270	344	446.5	325.5	436.2
31	114	.0144	201	367	220	377.6	17.1	118	.29	32 100	9.4	----	----	2140	.270	316	430.9	301	422.6
32	125	.0157	82.5	301.2	219	377	16.9	116	.03	20 700	6.1	----	----	2160	.272	304	424.3	294	418.7
33	125	.0157	85	302.6	218	376.5	16.3	112	.14	33 000	9.7	----	----	2090	.264	321.5	434	305.5	425.1
34	124	.0156	87.5	304	217.5	376.2	16.4	113	.19	39 000	11.4	----	----	2110	.266	344	446.5	325.5	436.2
35	175	.0221	200	366.5	219.5	377.3	17.0	117	.19	31 800	9.3	----	----	2170	.274	314.5	430.1	300	422
36	184	.0242	82.5	301.2	216	375.4	15.8	109	0	23 900	7.0	----	----	2150	.271	305	424.8	293.5	418.4
37	182	.0239	85	302.6	218.5	376.8	16.7	115	.04	30 900	9.1	----	----	2100	.265	326	436.5	311	428.2
38	181	.0238	87.5	304	218	376.5	16.5	114	.08	38 000	11.1	----	----	2060	.257	343	445.9	324.5	435.6
39	239	.0301	83	301.5	218.5	376.8	16.6	114	.01	32 100	9.4	----	----	2110	.266	327	437.1	311	428.2
40	239	.0301	83.5	301.8	219	377	16.8	116	.03	38 500	11.3	----	----	2090	.264	342.5	445.6	324	435.4
41	261	.0329	201	367	220	377.6	17.1	118	.12	33 600	9.6	----	----	2160	.272	316	430.9	300.5	422.3
42	356	.0448	199	366	220	377.6	17.1	118	.09	32 800	9.6	----	----	2050	.258	316	430.9	301	422.6
43	455	.0573	200.5	366.8	219.5	377.3	17.0	117	.06	32 300	9.5	----	----	2100	.265	315.5	430.6	299.5	421.8
44	518	.0652	120.5	322.3	218.5	376.8	16.7	115	.04	69 000	20	----	----	8520	1.07	329	438.2	321	433.7
45	518	.0652	155.5	341.8	219	377	16.8	116	.08	69 000	20	----	----	8520	1.07	329	438.2	321	433.7
46	518	.0652	185.5	358.4	220	377.6	17.1	118	.11	69 000	20	----	----	8520	1.07	329	438.2	321	433.7

<sup>a</sup>Length at which sudden rise in inner-wall temperature occurred.<sup>b</sup>Variation in boiling-fluid flowrate  $\pm 5$  to 10 percent.<sup>c</sup>Could not be determined accurately.

TABLE II. - Continued. EXPERIMENTAL DATA

## (b) Test section 1 - parallel flow

Run	Boiling fluid									Heating rate, Q		Critical length, <sup>a</sup> L <sub>C</sub>		Heating fluid					
	Flow rate, W <sub>B</sub>		Inlet temperature, T <sub>BI</sub>		Exit temperature, T <sub>BE</sub>		Exit pressure, P <sub>E</sub>		Exit quality, x <sub>E</sub>	Btu/hr	kW	ft	m	Flow rate, W <sub>H</sub>		Inlet temperature, T <sub>HI</sub>		Exit temperature, T <sub>HE</sub>	
	lb <sub>m</sub> /hr	kg/sec	°F	°K	°F	°K	psia	kN/m <sup>2</sup> (abs)						lb <sub>m</sub> /hr	kg/sec	°F	°K	°F	°K
1	50	0.0063	87.5	304	219	377	16.8	116	0.40	25 800	7.6	----	----	2110	0.266	302	423.2	289.5	416.2
2	50	.0063	90	305.4	219.5	377.3	17.0	117	.58	34 000	10.0	----	----	2100	.264	327	437.1	310	427.6
3	<sup>b</sup> 51	.0064	99	310.4	218.5	376.8	16.7	115	.67	39 600	11.6	2.50	0.762	2090	.263	348	448.7	329	438.2
7	67	.0084	88	304.3	219	377	16.9	116	.26	24 700	7.2	----	----	2120	.267	305	424.8	293	418.2
8	67	.0084	91	306	219	377	16.9	116	.41	35 200	10.3	----	----	2090	.263	326	436.5	309	427.1
10	<sup>b</sup> 85	.0107	93	307	221	378.2	17.4	120	.63	62 000	18	----	----	6260	.788	341	444.8	331	439.2
11	95	.0120	87	303.7	218.5	376.8	16.8	116	.15	25 800	10.5	----	----	2120	.267	306	425.9	293.5	418.4
12	96	.0121	89	304.8	219	377	16.9	116	.23	33 900	9.9	----	----	2080	.262	326.5	436.8	310	427.6
13	124	.0156	86	303.2	218.5	376.8	16.8	116	.09	27 500	8.1	----	----	2160	.272	307	425.9	294	418.7
14	124	.0156	88	304.3	219	377	16.9	116	.17	35 900	10.5	----	----	2100	.264	327	437.1	310	427.6
15	126	.0159	86	303.2	218.5	376.8	16.7	115	.19	39 800	11.7	----	----	2100	.264	343	445.9	324	435.4
16	181	.0228	85	302.6	219	377	16.9	116	.01	25 800	7.6	----	----	2120	.267	304.5	424.5	292	417.6
17	182	.0229	90	305.4	220.5	377.9	17.3	119	.07	35 500	10.4	----	----	2100	.264	327	437.1	310	427.6
18	183	.0230	83.5	301.8	218.5	376.8	16.6	114	.11	43 100	12.6	----	----	2100	.264	342	445.4	321.5	434
19	240	.0302	90	305.4	220	377.6	17.1	118	.02	35 400	10.4	----	----	2100	.264	327	437.1	310	427.6
20	239	.0301	83	301.5	220.5	377.9	17.2	118	.03	39 800	11.7	----	----	2100	.264	341	444.8	322	434.3

## (c) Test section 2 - countercurrent flow

Run	Boiling fluid											Heating rate, Q		Critical length, <sup>a</sup> L <sub>C</sub>		Heating fluid					
	Flow rate, W <sub>B</sub>		Inlet temperature, T <sub>BI</sub>		Exit temperature, T <sub>BE</sub>		Inlet pressure, P <sub>I</sub>		Exit pressure, P <sub>E</sub>		Exit quality, x <sub>E</sub>					Flow rate, W <sub>H</sub>		Inlet temper- ature, T <sub>HI</sub>		Exit temper- ature, T <sub>HE</sub>	
	lb <sub>m</sub> hr	kg sec	°F	°K	°F	°K	psia	kN m <sup>2</sup> (abs)	psia	kN m <sup>2</sup> (abs)	Btu hr	kW	ft	m	lb <sub>m</sub> hr	kg sec	°F	°K	°F	°K	
1	<sup>b</sup> 49	0.0060	145	336	148.5	337.9	8.1	56	3.6	25	0.88	44 000	13	1.75	0.533	7980	1.01	286	414.3	280.5	411.2
2	<sup>b</sup> 50	.0063	135	330.4	149.5	338.4	11.0	76	3.7	26	.88	44 000	13	1.25	.381	8060	1.01	344.5	446.8	339	443.7
3	<sup>b</sup> 62	.0078	113	318.2	155	341.5	8.5	59	4.2	29	.73	48 000	14	----	----	8200	1.03	256	397.6	250	394.3
4	61	.0077	106	314.3	150.5	339	10.5	72	3.8	26	.82	53 000	15	3.25	.990	8050	1.01	285.5	414	279	410.4
5	<sup>b</sup> 61	.0077	150	338.7	146	336.5	10.2	70	3.4	23	.78	48 000	14	2.25	.686	8010	1.01	315	433.4	309	427
6	<sup>b</sup> 63	.0079	135	330.4	157	342.6	13.0	90	4.0	28	1.0	68 000	20	1.75	.533	8080	1.02	342	445.6	333.5	440.6
7	71	.0089	115	319.3	156	342	15.5	107	4.3	30	.83	61 000	18	2.00	.610	8130	1.02	335.5	441.8	328	437.6
8	70	.0088	117	320.4	156	342	13.5	93	4.3	30	.93	68 000	20	2.25	.686	8100	1.02	339	443.7	331	439.2
9	78	.0098	107	314.8	155	341.5	11.2	77	4.2	29	.82	68 000	20	4.50	1.37	8050	1.01	287.5	415.1	279	410.4
10	79	.0099	108	315.4	160.5	344.3	13.5	93	4.8	33	.85	71 000	21	2.25	.686	8100	1.02	341	444.8	332	439.8
11	98	.0124	115	319.3	156	342	9.3	64	4.3	30	.45	48 000	14	----	----	8200	1.03	255.5	397.3	249.5	394
12	98	.0124	115	319.3	160.5	344.3	12.3	85	4.8	33	.65	69 000	20	----	----	8050	1.01	288.5	415.6	280	411
13	98	.0124	121	322.6	160.5	344.3	14.5	100	4.8	33	.77	80 000	23	4.25	1.30	8010	1.01	318.5	432.3	308.5	426.8
14	123	.0155	110	316.5	162	345.4	12.7	88	4.9	34	.50	68 000	20	----	----	8010	1.01	289.5	416.2	281	411.5
15	153	.0193	114	318.7	157	342.6	8.7	60	4.4	30	.24	43 000	13	----	----	8200	1.03	256	397.6	251	394.8

<sup>a</sup>Length at which sudden rise in inner-wall temperature occurred.<sup>b</sup>Variation in boiling-fluid flowrates  $\pm 5$  to 10 percent.

TABLE II. - Continued. EXPERIMENTAL DATA

(c) Continued. Test section 2 - countercurrent flow

Run	Boiling fluid											Heating rate, Q		Critical length, <sup>a</sup> L <sub>C</sub>		Heating fluid					
	Flow rate, W <sub>B</sub>		Inlet temperature, T <sub>BI</sub>		Exit temperature, T <sub>BE</sub>		Inlet pressure, P <sub>I</sub>		Exit pressure, P <sub>E</sub>		Exit quality, x <sub>E</sub>					Flow rate, W <sub>H</sub>		Inlet temperature, T <sub>HI</sub>		Exit temperature, T <sub>HE</sub>	
	lb m hr	kg sec	°F	°K	°F	°K	psia	kN m <sup>2</sup> (abs)	psia	kN m <sup>2</sup> (abs)		Btu hr	kW	ft	m	lb m hr	kg sec	°F	°K	°F	°K
16	155	0.0195	125	324.8	162.5	345.6	13.4	92	5.0	34	0.41	70 000	20	----	----	8050	1.01	289	415.9	280.5	411.2
17	240	.0303	125	324.8	158	343.2	8.7	60	4.5	31	.13	39 000	11.5	----	----	8110	1.02	255	397.1	250	394.3
18	374	.0472	115	319.3	159	343.7	8.9	61	4.6	32	.07	43 000	13	----	----	8110	1.02	256.5	397.9	251	394.8
19	586	.0739	119	321.5	160	344.3	9.0	62	4.7	32	.04	46 000	13.5	----	----	8110	1.02	256.5	397.9	250.5	394.6
20	864	.109	116	319.8	160.5	345.6	8.5	59	4.8	33	.02	56 000	16.5	----	----	8110	1.02	257.5	398.4	250.5	394.6
21	864	.109	79.5	299.5	152	339.8	7.4	51	3.9	27	.002	64 000	19	----	----	8020	1.01	256	397.6	248	393.2
22	88	.0111	96	308.7	165.5	347.3	14.5	100	5.4	37	.77	74 000	21.5	3.00	0.915	8100	1.02	338	443.2	329	438.2
23	97	.0122	91	306	169	349.3	16.0	110	5.8	40	.84	88 100	25.8	3.50	1.07	8100	1.02	338.5	443.5	328	437.6
24	110	.0139	109	316	173.5	351.8	18.0	124	6.5	45	.78	92 400	27.1	4.00	1.22	8100	1.02	340.5	444.6	329.5	438.4
25	121	.0153	106	314.3	175.5	352.9	18.0	124	6.8	47	.71	93 700	27.3	4.50	1.37	8060	1.02	340	444.3	328.5	437.9
26	154	.0194	120.5	322.3	171.5	350.6	17.0	117	6.2	43	.48	81 800	24.0	----	----	8010	1.01	317.5	431.8	307.5	426.2
27	239	.0302	108	315.4	165	347	13.0	90	5.3	37	.21	64 000	19	----	----	8010	1.01	288	415.4	280	420.9
28	375	.0473	106	314.3	169	349.3	12.3	85	5.9	41	.12	69 000	20.5	----	----	8010	1.01	289.5	416.2	281	411.5
29	582	.0734	112	317.6	171.5	350.6	11.8	81	6.2	43	.06	68 000	20	----	----	8010	1.01	289	415.9	280.5	411.2
30	859	.108	78	298.7	176	353.2	12.0	83	6.9	48	.10	99 000	29.0	----	----	8110	1.02	322.5	434.6	312.5	429
31	b <sub>53</sub>	.0067	130	327.6	184	357.6	12.4	86	8.2	57	.73	41 000	12	1.75	.533	7990	1.01	304.5	424.5	299.5	421.8
32	b <sub>53</sub>	.0067	115	319.3	183.5	357.3	12.0	83	8.1	56	.88	50 000	14.5	2.75	.840	8010	1.01	291.5	417.5	285	413.7
33	b <sub>52</sub>	.0066	115	319.3	184	357.6	11.9	82	8.2	57	.54	31 000	9.2	2.00	.610	8010	1.01	289	415.9	285	413.7
34	57	.0072	110	316.5	184	357.6	12.5	86	8.2	57	.85	52 000	15	2.75	.840	8020	1.01	290	416.5	283.5	412.9
35	b <sub>58</sub>	.0073	110	316.5	184	357.6	11.8	81	8.2	57	.57	37 000	11	2.50	.762	7980	1.00	300.5	422.3	296	419.8
36	b <sub>51</sub>	.0064	160	344.3	183	357	12.0	83	8.0	55	.95	49 000	14.5	1.50	.457	8120	1.02	321	433.7	315	430.4
37	100	.0126	81	300.4	183	357	10.5	72	8.0	55	.06	16 000	4.7	----	----	8380	1.06	226	381	224	379.8
38	100	.0126	84	302	184	357.6	11.0	76	8.2	57	.26	35 000	10.5	----	----	8010	1.01	254	396.5	249.5	394
39	99	.0125	85	302.6	183	357	13.5	93	8.0	55	.58	66 000	19.5	----	----	8040	1.01	288.5	415.6	280.5	411.2
40	99	.0125	90	305.4	183	357	15.6	108	8.0	55	.85	82 200	24.1	4.50	1.37	7920	1.00	320.5	433.4	310	427.6
41	100	.0126	92.5	306.8	183	357	16.5	114	8.0	55	.85	83 500	24.5	3.75	1.14	7970	1.00	340.5	444.5	330	438.7
42	100	.0126	188.5	360.1	177	353.7	9.4	65	7.0	48	.26	24 000	7.0	----	----	8190	1.03	228	382	225	380.4
43	99	.0125	191	361.5	178	354.3	11.3	78	7.2	50	.42	40 000	12	----	----	8100	1.02	255	397.1	250	394.3
44	97	.0122	206	369.8	181	356	13.7	95	7.7	53	.58	53 000	15.5	----	----	8040	1.01	285.5	414	279	410.4
45	96	.0121	205	369.3	181	356	15.0	103	7.7	53	.80	73 000	21.5	4.00	1.22	8010	1.01	318.5	432.3	309.5	427.3
46	100	.0126	205	369.3	181.5	356.2	17.0	117	7.8	54	.85	82 000	24.0	2.50	.762	7990	1.01	341	444.8	331	439.3
47	200	.0252	75	297	183.5	357.3	11.3	78	8.1	56	.06	34 000	9.9	----	----	8060	1.01	254.5	396.8	250	394.3
48	201	.0253	75	297	183	357	14.0	97	8.0	55	.20	61 000	18	----	----	8050	1.01	288.5	415.6	281	411.5
49	199	.0251	77	298.2	184	357.6	17.1	118	8.2	57	.33	87 300	25.6	----	----	7970	1.00	321.5	434	310.5	427.9
50	197	.0248	79	299.3	183.5	357.3	20.5	141	8.1	56	.42	103 000	30.1	----	----	8020	1.01	343	445.9	330.5	439
51	204	.0257	220	377.6	187	359.2	25.2	174	8.7	60	.53	99 300	29.1	----	----	8050	1.01	342	445.4	330	438.7
52	153	.0193	118.5	321.2	183	357	21.0	145	8.0	55	.63	105 000	30.7	----	----	8060	1.01	342.5	445.6	330	438.7
53	195	.0246	119	321.5	187	359.2	21.7	149	8.7	60	.47	103 000	30.4	----	----	8100	1.02	342.5	445.6	330	438.7
54	244	.0308	126.5	325.6	188	359.8	22.5	155	8.9	61	.35	99 800	29.2	----	----	8100	1.02	341	444.8	329	438.2
55	295	.0372	125	324.8	190	361	22.5	155	9.3	64	.27	98 500	28.9	----	----	8100	1.02	342.5	445.6	330.5	439

<sup>a</sup>Length at which sudden rise in inner-wall temperature occurred.<sup>b</sup>Variation in boiling-fluid flowrates  $\pm 5$  to 10 percent.



TABLE II. - Concluded. EXPERIMENTAL DATA

(c) Concluded. Test section 2 - countercurrent flow

Run	Boiling fluid										Heating rate, Q		Critical length, <sup>a</sup> L <sub>C</sub>		Heating fluid						
	Flow rate, W <sub>B</sub>		Inlet temperature, T <sub>BI</sub>		Exit temperature, T <sub>BE</sub>		Inlet pressure, P <sub>I</sub>		Exit pressure, P <sub>E</sub>						Exit quality, x <sub>E</sub>	Flow rate, W <sub>H</sub>		Inlet temper- ature, T <sub>HI</sub>		Exit temper- ature, T <sub>HE</sub>	
	lb m hr	kg sec	°F	°K	°F	°K	psia	kN m <sup>2</sup> (abs)	psia	kN m <sup>2</sup> (abs)	Btu hr	kW	ft	m		lb m hr	kg sec	°F	°K	°F	°K
56	238	0.0300	128	326.5	179	354.8	17.9	123	7.1	49	0.29	82 400	23.9	----	----	8010	1.01	318.5	432.3	308.5	426.8
57	377	.0475	127.5	326.2	182	356.2	17.8	123	7.9	54	.16	81 800	24.0	----	----	8050	1.01	318.5	432.3	308.5	426.8
58	580	.0731	126	325.4	187	359.3	16.7	115	8.7	60	.09	84 100	24.7	----	----	8050	1.01	319	432.6	308.5	426.8
59	858	.108	135	330.4	188	359.8	16.4	113	8.9	61	.05	84 200	24.7	----	----	8010	1.01	318.5	432.3	308	426.5
60	860	.108	130.5	327.9	179	354.8	12.9	89	7.4	51	.04	74 000	22	----	----	7980	1.00	290.5	416.8	281.5	411.8
61	99	.0125	85	302.6	202	367.6	13.7	95	12.0	83	.16	27 000	8.0	----	----	7980	1.00	253.5	396.2	250	394.3
62	101	.0127	85	302.6	202	367.6	15.4	106	12.0	83	.45	56 000	16.5	----	----	8040	1.01	287.5	415.1	280.5	411.2
63	99	.0125	88.5	304.6	202	367.6	17.4	120	12.0	83	.70	79 000	23	4.00	1.22	8010	1.01	320	433.2	310.5	427.9
64	99	.0125	90	305.4	202	367.6	18.0	124	12.0	83	.78	89 000	26.1	3.50	1.07	7880	.994	340.5	444.5	329.5	438.4
65	99	.0125	200	366.5	200	366.5	13.3	92	11.5	79	.28	27 000	8.3	----	----	8000	1.01	253.5	396.2	250	394.3
66	97	.0122	203	368.2	201	367	15.7	108	11.7	81	.59	56 000	16.5	----	----	7960	1.00	289	415.9	282	412
67	100	.0126	216.5	375.6	197	364.8	16.7	115	10.1	70	.68	64 000	19	3.00	.914	8000	1.01	319	432.6	311	428.2
68	100	.0126	219	377	197.5	365.1	17.2	118	11.0	76	.78	74 000	21.7	2.75	.839	8000	1.01	342.5	445.6	333.5	440.6
69	371	.0468	141	333.7	194	363.2	23.7	163	10.2	70	.23	98 800	29.0	----	----	8060	1.02	342.5	445.6	330.5	439
70	581	.0732	137	331.5	200	366.5	22.5	155	11.5	79	.12	104 000	31.4	----	----	8100	1.02	342.5	445.6	330	438.7
71	855	.107	143	334.8	205	369.3	22.2	153	12.8	88	.06	98 800	29.0	----	----	8060	1.02	344.5	446.8	332.5	440.1
72	861	.108	86	303.2	190	360	15.7	108	9.3	64	.03	118 000	35.8	----	----	8150	1.03	344.5	446.8	330.5	439
73	100	.0126	69	293.7	218.5	376.8	18.3	126	16.6	114	.29	41 000	12	----	----	8040	1.01	286.5	414.5	281	411.5
74	100	.0126	70	294.3	219	377	20.5	141	16.8	116	.64	76 000	22	----	----	7910	.997	319.5	432.9	310	427.6
75	100	.0126	74	296.5	219.5	377.3	21.7	149	17.0	117	.83	94 400	27.6	4.50	1.37	7890	.994	340.5	444.5	329.5	438.4
76	98	.0124	199	365.9	218.5	376.8	17.7	122	16.7	115	.11	11 000	3.3	----	----	8020	1.01	250.5	394.5	249	393.7
77	100	.0126	198	365.4	218.5	376.8	18.7	129	16.7	115	.43	42 000	12.5	----	----	7910	.997	286.5	414.5	281.5	411.8
78	99	.0125	204	368.7	219.5	377.3	21.3	147	17.0	117	.67	65 000	19	----	----	8000	1.01	318	432	310	427.6
79	102	.0128	210	372	220	377.6	22.2	153	17.2	118	.80	80 000	23.5	3.00	.914	8020	1.01	342	445.4	332	439.8
80	100	.0126	68	293.2	238.5	387.9	25.8	178	24.1	166	.10	26 000	7.6	----	----	8010	1.01	283.5	412.5	280	410.9
81	99	.0125	72	295.4	237.5	387.3	25.8	178	23.8	164	.50	64 000	18.5	----	----	8000	1.01	319.5	432.9	311.5	428.4
82	100	.0126	74	296.5	238	387.6	27.0	186	24.0	165	.66	79 000	23.2	----	----	7880	.993	340	444.3	330	438.7
83	98	.0124	230	383.2	237.5	387.3	24.5	169	23.7	163	.30	29 000	8.4	----	----	8070	1.02	282.5	412.3	279	410.4
84	99	.0125	229	382.6	238	387.6	26.5	183	24.0	165	.68	65 000	19	----	----	8000	1.01	320	433.2	312	428.7
85	101	.0127	229	382.6	238	387.6	27.5	189	24.0	165	.89	87 000	25.5	4.50	1.37	8020	1.01	342.5	445.6	332	439.8
86	50	.0063	85	302.6	180	355.4	9.4	65	7.5	52	.26	18 000	5.2	----	----	4020	.507	230.5	383.4	226	381
87	50	.0063	88	304.3	181	355.9	10.0	69	7.7	53	.56	33 000	9.7	----	----	4060	.512	259	399.3	250.5	394.5
88	50	.0063	103	312.6	183	357	10.7	74	8.0	55	.91	49 300	14.5	3.50	1.07	4030	.508	290.5	416.8	278	409.8
89	50	.0063	110	316.5	183.5	357.3	11.9	82	8.1	56	.99	52 400	15.4	3.25	.990	4030	.508	303	423.7	290	416.5

<sup>a</sup>Length at which sudden rise in inner-wall temperature occurred.<sup>b</sup>Variation in boiling-fluid flowrates  $\pm 5$  to 10 percent.

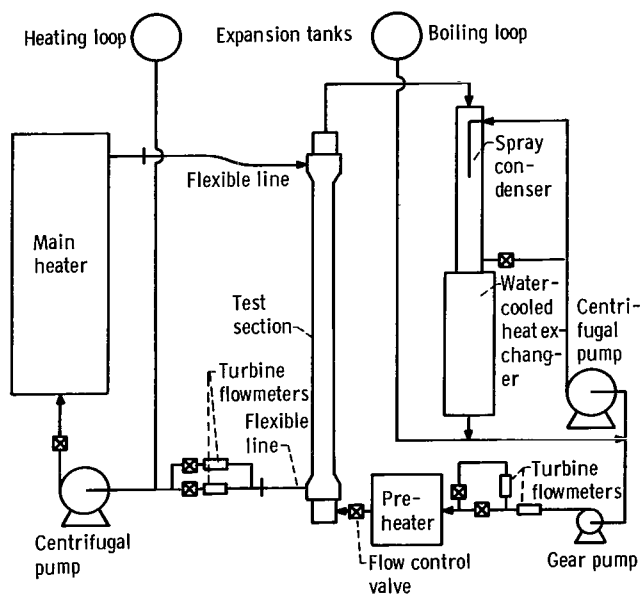
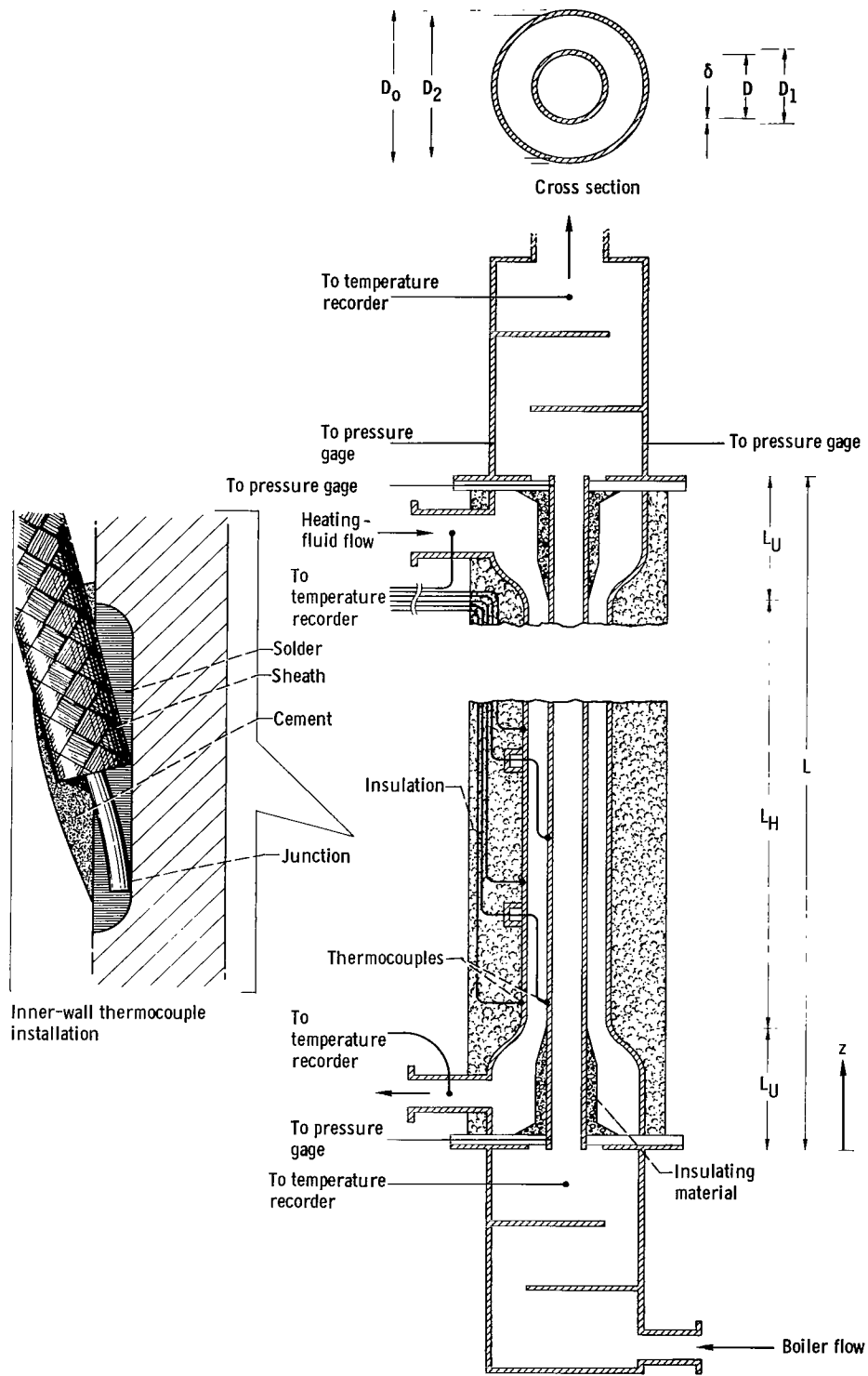


Figure 1. - Schematic diagram of test rig.



CD-9034

Figure 2. - Diagram of test section and plenum chambers.

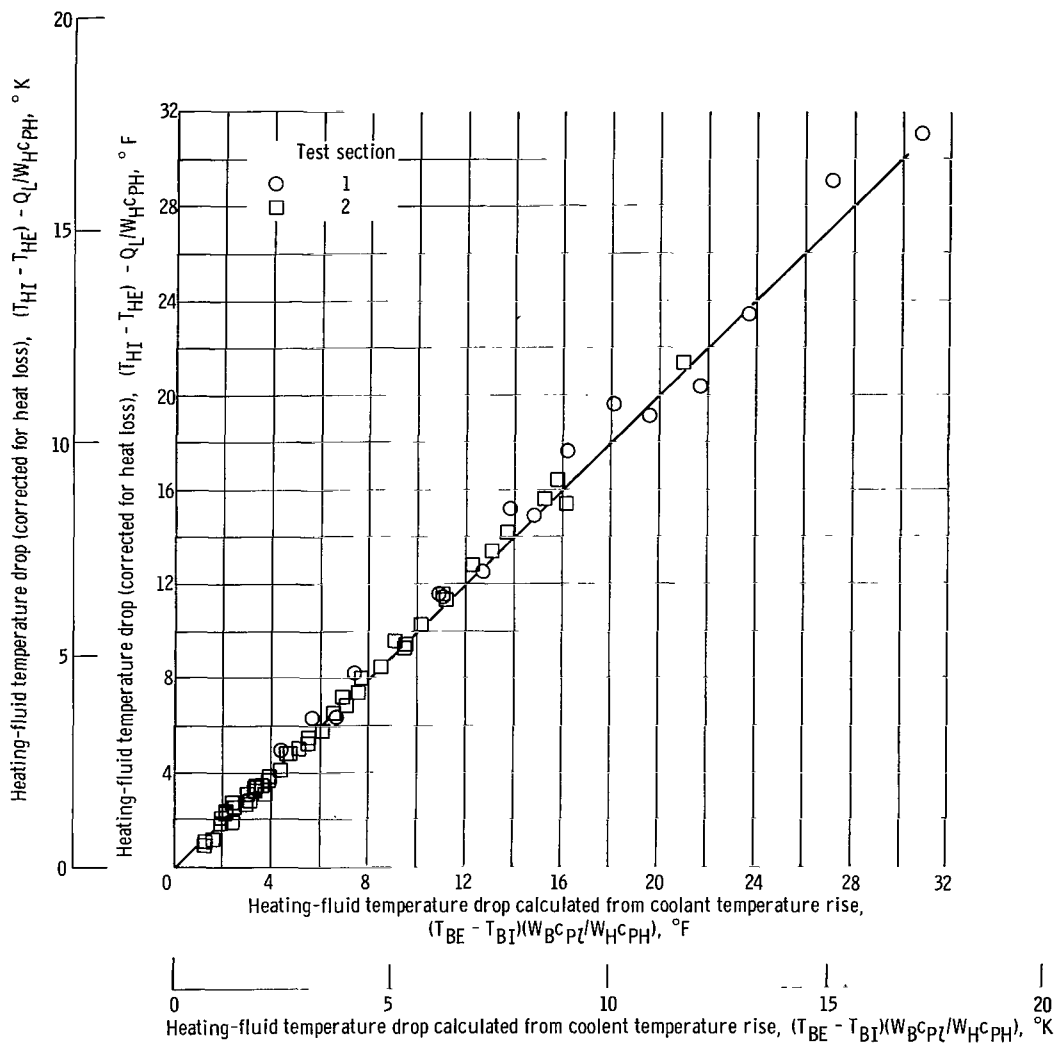


Figure 3. - Comparison of heating-fluid temperature drop (corrected for heat loss) with that computed from coolant temperature rise.

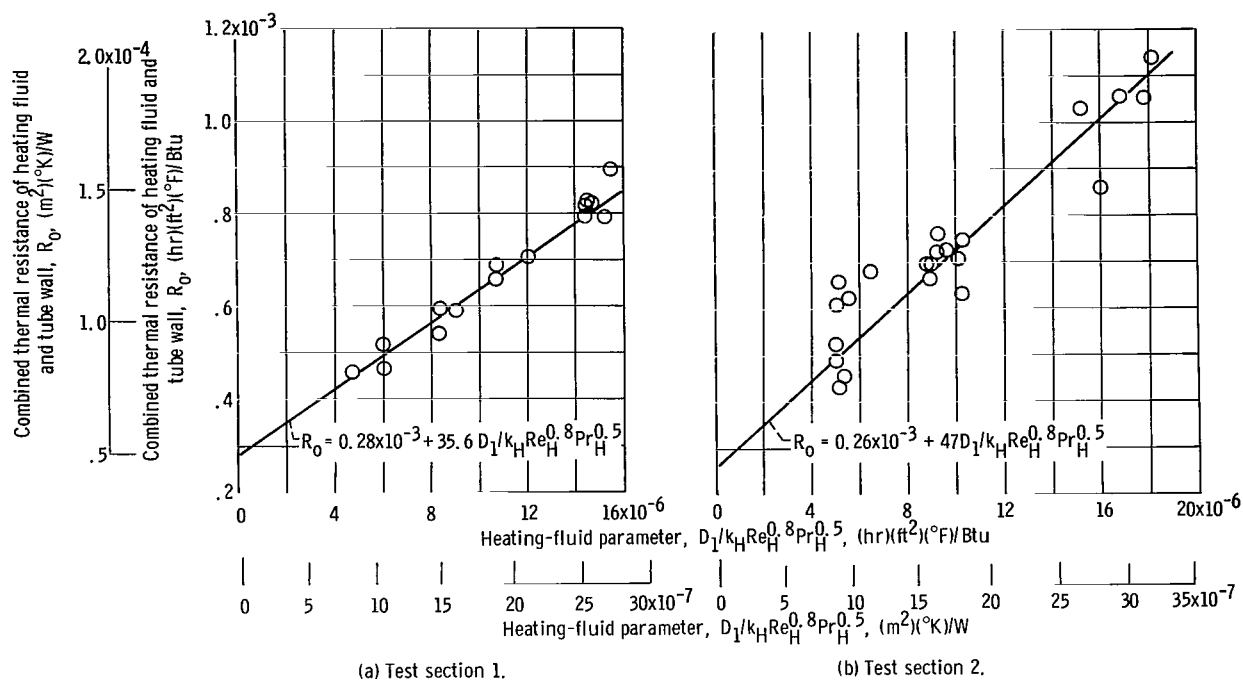


Figure 4. - Determination of wall and heating-fluid thermal resistance  $R_0$ .

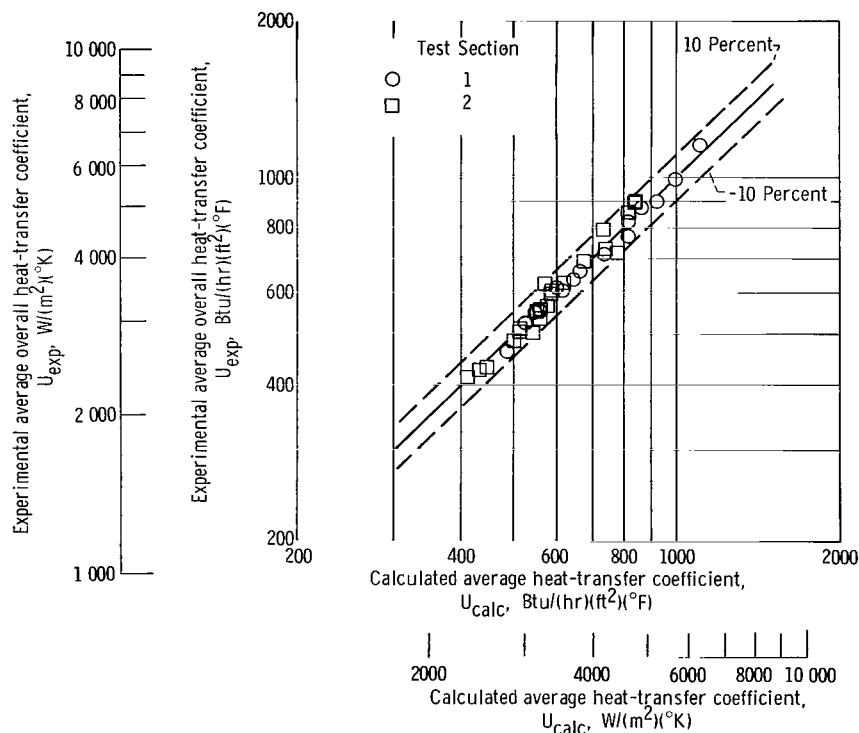


Figure 5. - Comparison of experimental and calculated values of average overall heat-transfer coefficient  $U$ . (Nonboiling calibration runs.)

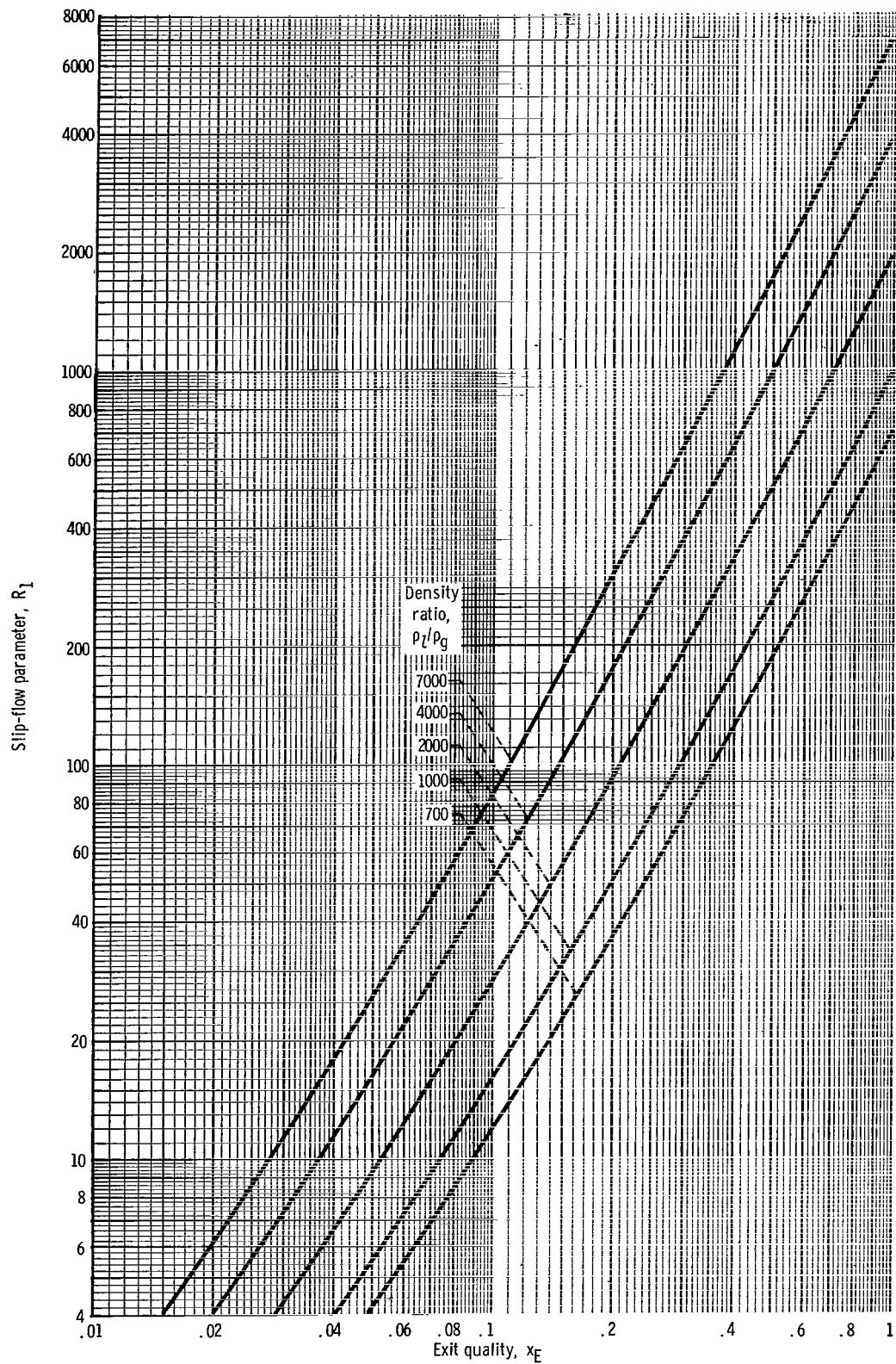


Figure 6. - Slip-flow parameter  $R_1$  as function of exit quality for various values of density ratio.

$$R_1 = [1 + (\sqrt{\rho_L/\rho_g} - 1)x_E]^2 - 1.$$

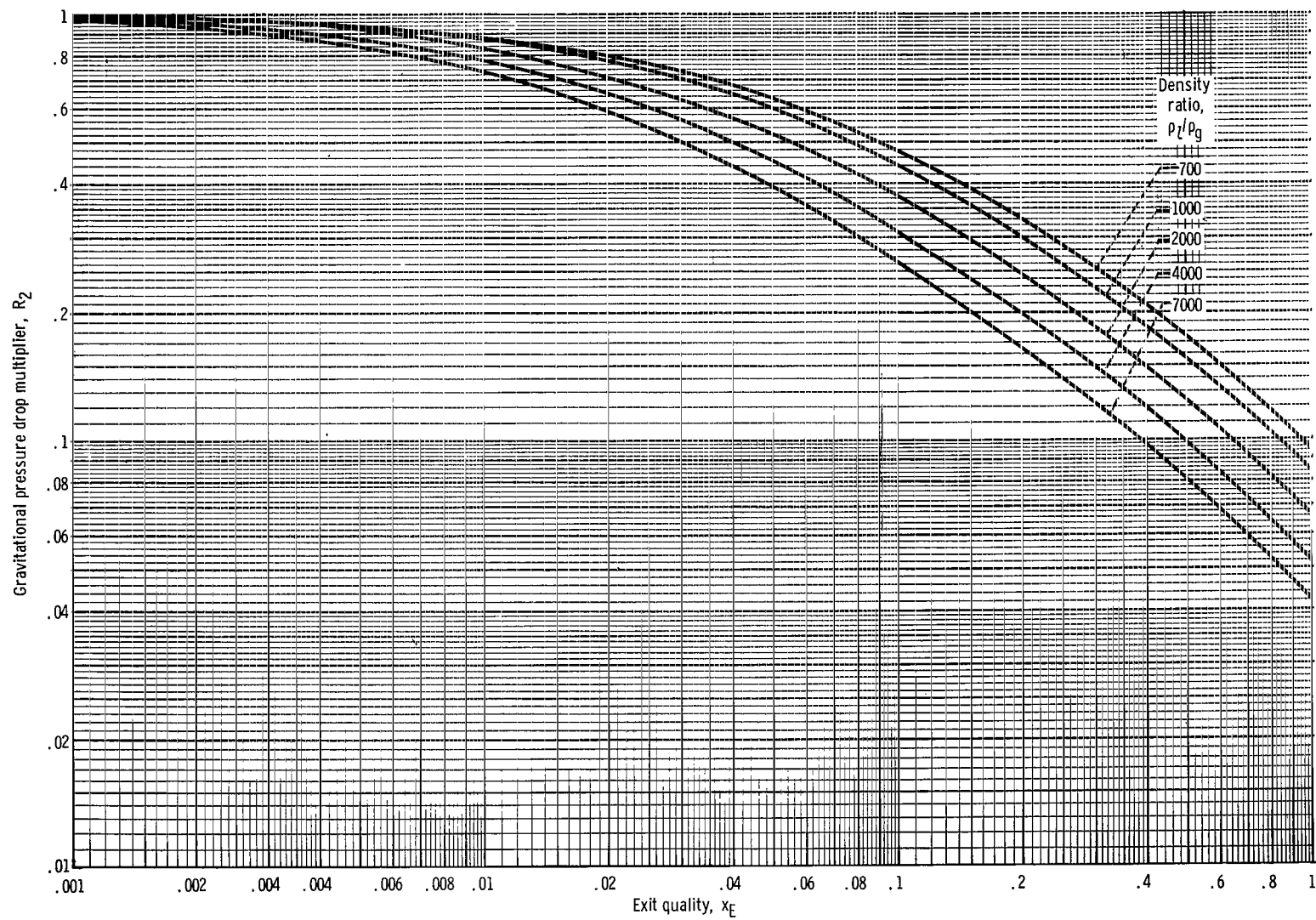


Figure 7. - Gravitational pressure drop multiplier  $R_2$  as function of exit quality for various values of density ratio.

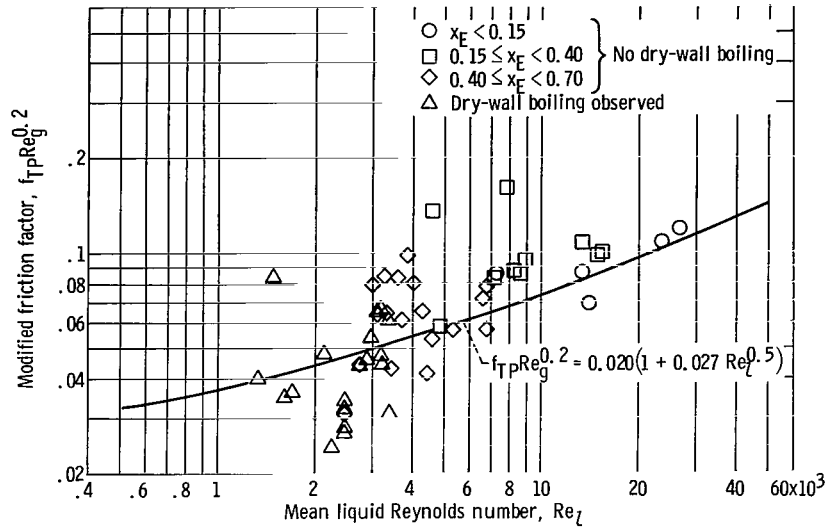


Figure 8. - Correlation of two-phase friction factor as function of mean Reynolds numbers of liquid and vapor.

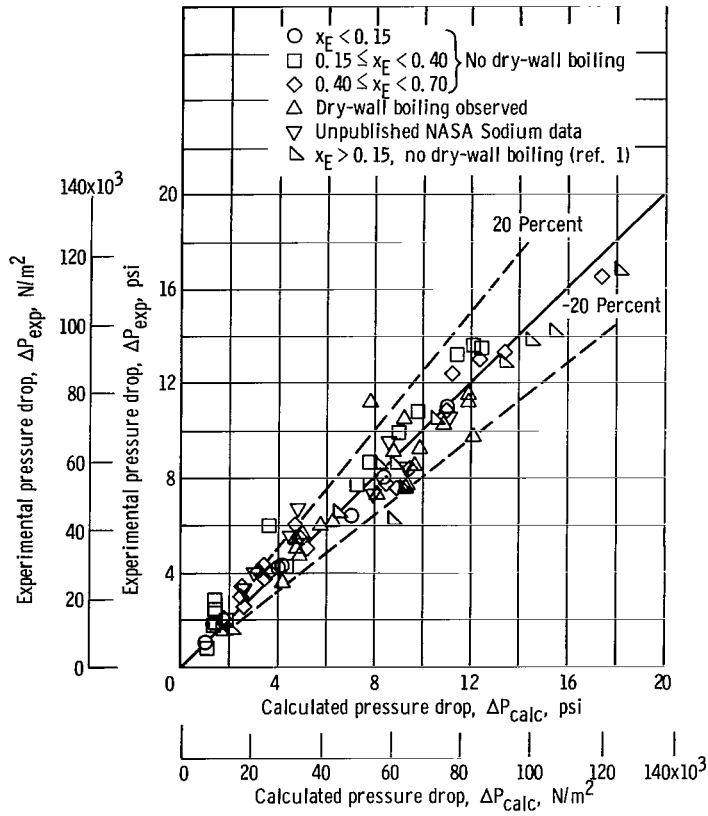


Figure 9. - Comparison of experimental pressure drop data with values calculated from equations (14) and (17); exit quality,  $>1.5 c_{pL}(T_{SE} - T_{BI})/\lambda_1$ ; boiler flow rate,  $>60$  pounds (mass) per hour (0.0076 kg/sec).

$$\Delta P_{\text{calc}} = R_2 \rho_L L_H \left( \frac{g}{g_c} \right) + \frac{R_1 G^2}{\rho_L g_c} + 0.020 \text{Re}_g^{-0.2} (1 + 0.027 \text{Re}_L^{0.5}) (R_1 + 2) \frac{G^2 L_H}{\rho_L g_c D}$$



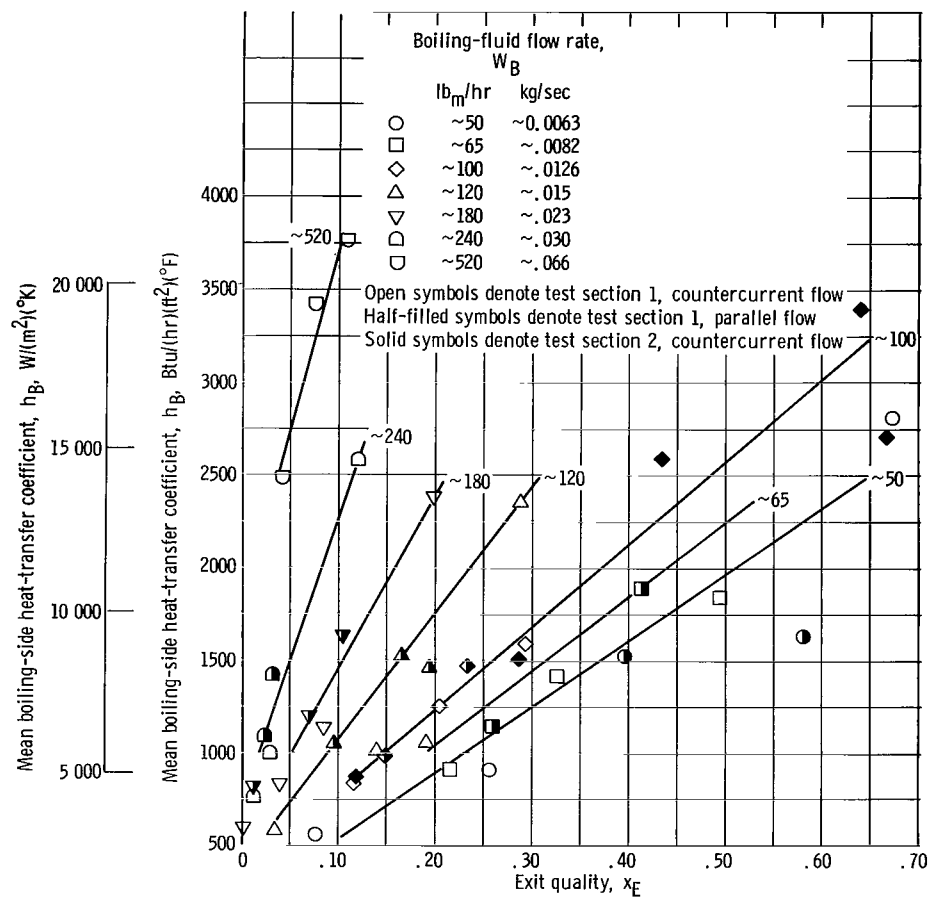


Figure 10. - Mean boiling-side heat-transfer coefficient as function of exit quality for various boiling-fluid flowrates. Exit pressure, ~17 pounds per square inch absolute (~115 kN/m<sup>2</sup>); no dry-wall boiling.

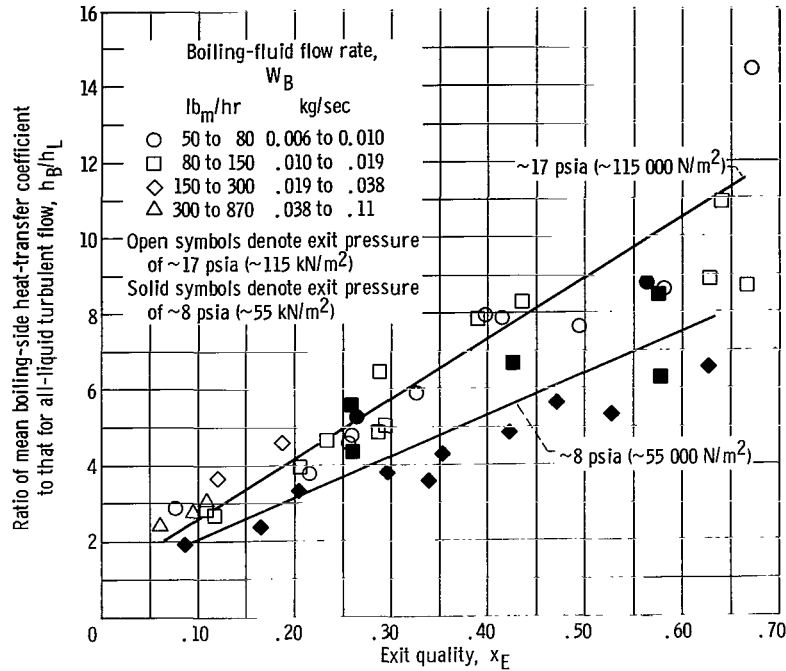


Figure 11. - Ratio of mean boiling-side heat-transfer coefficient to that for all-liquid turbulent flow as function of exit quality for exit pressures of ~8 and ~17 pounds per square inch absolute (~55 and ~115 kN/m<sup>2</sup>), no dry-wall boiling, and  $x_E > 1.5 c_{PL}(T_{SE} - T_{BI})/\lambda$ .

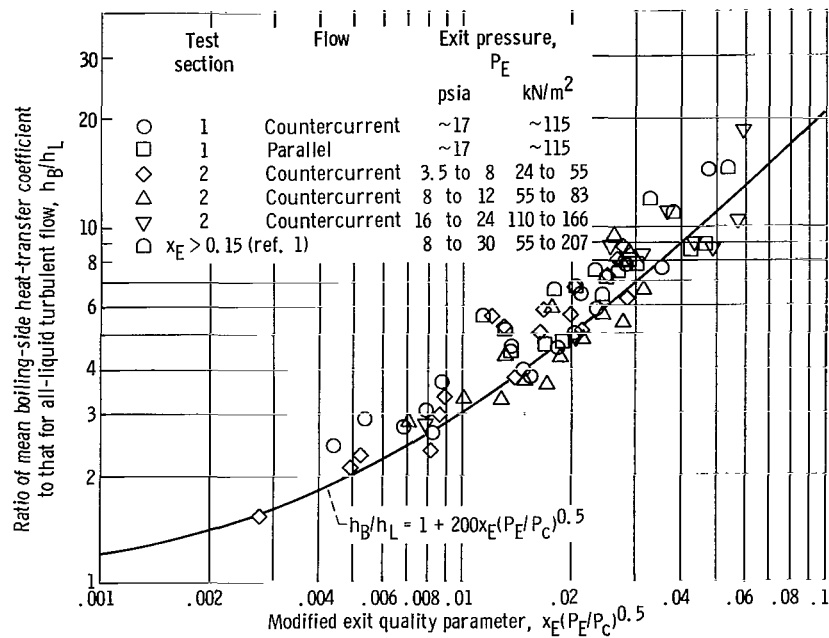


Figure 12. - Ratio of mean boiling-side heat-transfer coefficient to that for all-liquid turbulent flow as function of exit quality and pressure for no dry-wall boiling and exit quality greater than  $1.5 c_{PL}(T_{SE} - T_{BI})/\lambda$ .

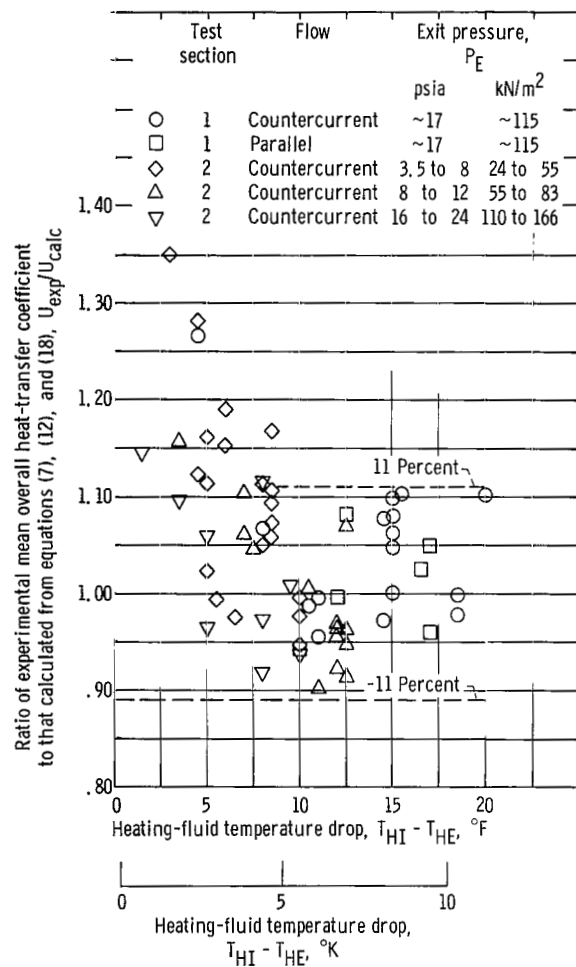


Figure 13. - Ratio of experimental mean overall heat-transfer coefficient to that calculated for experimentally determined exit quality compared to heating-fluid temperature drop; no dry-wall boiling; and exit quality greater than  $1.5 c_{pL}(T_{SE} - T_{BT})/\lambda$ .

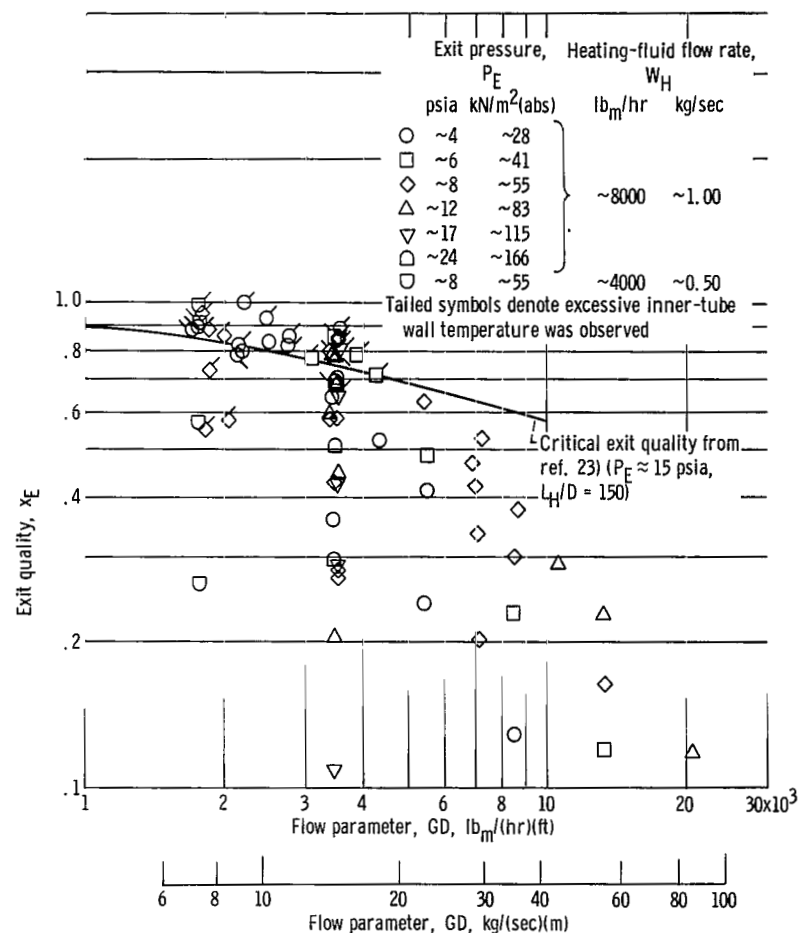


Figure 14. - Critical exit quality as function of flow parameter  $GD$ . Test section 2;  $L_H/D = 139$ .

*"The aeronautical and space activities of the United States shall be conducted so as to contribute . . . to the expansion of human knowledge of phenomena in the atmosphere and space. The Administration shall provide for the widest practicable and appropriate dissemination of information concerning its activities and the results thereof."*

—NATIONAL AERONAUTICS AND SPACE ACT OF 1958

## NASA SCIENTIFIC AND TECHNICAL PUBLICATIONS

**TECHNICAL REPORTS:** Scientific and technical information considered important, complete, and a lasting contribution to existing knowledge.

**TECHNICAL NOTES:** Information less broad in scope but nevertheless of importance as a contribution to existing knowledge.

**TECHNICAL MEMORANDUMS:** Information receiving limited distribution because of preliminary data, security classification, or other reasons.

**CONTRACTOR REPORTS:** Scientific and technical information generated under a NASA contract or grant and considered an important contribution to existing knowledge.

**TECHNICAL TRANSLATIONS:** Information published in a foreign language considered to merit NASA distribution in English.

**SPECIAL PUBLICATIONS:** Information derived from or of value to NASA activities. Publications include conference proceedings, monographs, data compilations, handbooks, sourcebooks, and special bibliographies.

**TECHNOLOGY UTILIZATION PUBLICATIONS:** Information on technology used by NASA that may be of particular interest in commercial and other non-aerospace applications. Publications include Tech Briefs, Technology Utilization Reports and Notes, and Technology Surveys.

*Details on the availability of these publications may be obtained from:*

SCIENTIFIC AND TECHNICAL INFORMATION DIVISION  
NATIONAL AERONAUTICS AND SPACE ADMINISTRATION  
Washington, D.C. 20546